2019-01-01

An Alternative Method Of Calibration And Prediction For The Theta-Projection Model

Jimmy Jesus Perez
University of Texas at El Paso, jimmyjperez16@gmail.com

AN ALTERNATIVE METHOD OF CALIBRATION AND PREDICTION FOR THE THETA-PROJECTION MODEL

JIMMY JESUS PEREZ

Master's Program in Mechanical Engineering

APPROVED:

Calvin M. Stewart, Ph.D., Chair

Jack F. Chessa, Ph.D

Soheil Nazarian, Ph.D.

Charles Ambler, Ph.D.
Dean of the Graduate School

DEDICATION

Dedicated to my grandfather.
Jose Perez

AN ALTERNATIVE METHOD OF CALIBRATION AND PREDICTION FOR THE THETA PROJECTION MODEL

by

JIMMY JESUS PEREZ, B.Sc.

THESIS

Presented to the Faculty of the Graduate School of

The University of Texas at El Paso

in Partial Fulfillment

of the Requirements

for the Degree of

MASTER OF SCIENCE

Department of Mechanical Engineering

THE UNIVERSITY OF TEXAS AT EL PASO

May 2019

ACKNOWLEDGEMENTS

I would like to thank my advisor Dr. Calvin Stewart for his insight and guidance through my undergraduate and graduate degree. I would also like to thank my family, friends and loved ones for their continual support and encouragement through this long journey.

ABSTRACT

The combustion induced high temperature-stress conditions of industrial gas turbines used in power generation causes turbine blades to wear and break after prolonged use. The need to predict turbine blade service life is ever increasing, leading to the development of several constitutive prediction models. It is necessary to design components for high-temperature/high-stress service such that creep failure does not occur during service life. For this reason, it is important to accurately predict creep life and understand the behavior of creep deformation leading to rupture. Several models have been expanded upon to improve their effectiveness for use with particular parametric data. One such model, popular for its flexibility, is the theta-projection model. The theta-projection model, developed by R. W. Evans in response to the point-prediction limitations of previous models, excels at fitting the graphical form of creep deformation plotted with time. The method of application proposed by Evans for interpolating and extrapolating predictions of creep deformation requires that the model constants be optimized using a least-square non-linear scheme with respect to an error function. These numerically optimized constants are used to establish an interpolation and extrapolation formula of temperature and stress. Once the interpolation/extrapolation formula has been established, theta constants can be derived for any temperature-stress condition. Though this form of numerical optimization generates constants that produce excellent fits to experimental data, the principal issue is that the numerical optimization process does not produce constants with a trend that is conducive to the interpolation/extrapolation formula. Using the proposed interpolation function, variations from constant to constant cause imprecise predictions. To address this prediction issue, three alterations to the theta projection method are proposed. Firstly, it is necessary to implement a method of calibration that produces a consistent, physically realistic trend of theta constants for use in prediction. An analytical approach

to calibration is used to derive theta constants with respect to the experimental data used in calibration. As the behavior of the data changes with temperature and stress, so do the theta constants in a similar, more consistent manner. Secondly, an alternative interpolation/extrapolation function that relies on rupture time rather than temperature and stress is used to make predictions. The rupture time of test data follows a pattern as stress and temperature change. The theta-rupture time relationship results in more precise predictions than the original theta-stress/temperature relationship. Thirdly and finally, it is necessary to relate the rupture time to temperature and stress so that any prediction at desired conditions can be made. The Wilshire model includes an equation relating rupture time to temperature and stress. Applying this Wilshire equation is the final step in the modified theta-projection method. The modified theta-projection method is demonstrated using a database of creep deformation data for Alloy P91. It is determined that the method provides more reliable calibration, better functionalization, and predictions that are on par with the original theta method while requiring less constants to be calibrated.

TABLE OF CONTENTS

LIST OF TABLES

LIST OF FIGURES

CHAPTER 1: INTRODUCTION

1.1 MOTIVATION

As the demand for higher efficiency in power generation increases, so do the operating conditions for industrial gas turbines. Subject to high-temperature, high-stress conditions, turbine blades are subject to fretting, creep-fatigue and ductility-fracture. Higher service conditions shorten service life; therefore, it is necessary to characterize the performance of different alloys and design the blades accordingly. Some methods to determine the behavior of different alloys when subject to parametric conditions of temperature and stress over time is via creep and stress-relaxation. It is through creep tests that creep deformation, rupture, and minimum-creep-strain-rate data is collected. Studying the behavior of creep data and making predictions based on said data is done via creep prediction models, of which many have been developed [1-3]. Moreover, these models are applied in Finite element analysis to predict the performance of components and redesign them or select different alloys in order to meet design requirements. There are instances when academic research results in modified versions of these models to address a specific area of study or to improve the application of said model. The focus of this study is to improve the application of the theta-projection model when used to predict the creep deformation behavior of a specified alloy. The goal in conducting this research is to improve the methods of prediction for use in part design. Improved accuracy in prediction results in a better understanding of the behavior of the material when subject to parametric conditions.

The traditional method of calibration described by Evans for the theta-projection model is through numerical optimization. The issue with numerical optimization is that it relies only on an error function of a calibrated fit to experimental data. Very rarely is consideration given to the physical realism of the constants being optimized. Different combinations of the material constant

values my result in acceptable fits. This method may result in theta values that have no correlation to one another across isotherms or isostresses. This results in difficulty functionalizing them later in the prediction process.

1.2 APPROACH

The approach for implementing the alternative application technique for the theta projection model is a multi-step process. It begins with the model itself, the theta projection model is separated by regime into two distinct time-hardening and time-softening equations respectively [4-7]. Each of the four theta constants are phenomenologically and mathematically related to the shape of the creep curve section governed by their respective equation. The resulting constants are related to rupture time via a proposed set of interpolation/extrapolation interpolation/extrapolation functions that take a power-law form and rely on two constants. Rupture is predicted using the temperature- and stress-dependent Wilshire equation [8-11]. Using the rupture prediction and interpolation/extrapolation functions, the theta constants are generated for any combination of stress and temperature. Finally, creep deformation predictions are achieved.

1.3 ORGANIZATION

CHAPTER 2: BACKGROUND

is a background section, discussing the theta-projection model and the nuances of how it is intended to be used to fit creep test data and make interpolated and extrapolated predictions. Creep deformation as a phenomenon and its stages are introduced and the behavior as it differs with temperature and stress is explained. The Theta-projection model is introduced [4-7]. The original method of application for the theta projection model is explained [12]. The benefits and shortcomings of the theta projection technique are briefly addressed and are elaborated on in the

following chapters. A brief overview of history, properties, and composition of alloy P91 is discusses, followed by a description of the sets of P91 test data used in this work.

CHAPTER 3: THETA-PROJECTION PERFORMANCE REVIEW

demonstrates the performance of Theta-projection using the conventional calibration approach and interpolation/extrapolation functions. The existing method of calibration proposed by Evans is implemented on 3 sets of alloy P91 test data. A numerical optimization scheme is used to calibrate theta projection constants. The error of calibration and resulting interpolated predictions is assessed and discussed.

CHAPTER 4: ANALYTICAL CALIBRATION TECHNIQUE

introduces a new analytical calibration approach that addresses the issues elucidated in the previous CHAPTER 3: THETA-PROJECTION PERFORMANCE REVIEW

. The theta-projection model is broken down by regime and the material constants are related to the phenomenon of the classical creep curve. The analytical approach is compared to calibration by numerical optimization. Interpolated and extrapolated predictions are made using both methods of calibration and are compared to experimental data. Error of the two predictions are compared and discussed. It is determined that the analytical approach produces theta constants that exhibit a realistic trend as stress changes, which produces better interpolated and extrapolated predictions.

CHAPTER 5: ALTERNATIVE INTERPOLATION/EXTRAPOLATION FUNCTION STUDY

introduces new interpolation/extrapolation functions based on rupture. The analytical calibration method is applied to a set of data and the resulting theta constants are functionalized using the interpolation/extrapolation function established by Evans [4-7]. Theta constant values

are derived from the interpolation/extrapolation function. The temperature-stress parameters used to derive theta constants are the same as those used in calibration. The resulting predictions are compared to calibration data. Next, the process is repeated using the new interpolation/extrapolation function. The normalized mean square error (NMSE) for the creep deformation predictions of each interpolation/extrapolation function is compared. It is found that the new interpolation/extrapolation function produces better predictions than the original when using the same rupture time as validation data. The study is repeated using two different means of determining rupture time for each method of interpolation/extrapolation. Rupture time predicted using a Wilshire equation is used to make predictions with the new interpolation/extrapolation equation. Rupture time at 8% strain is used to make predictions with the original interpolation/extrapolation equation. The conventional interpolation/extrapolation functions are parametric surface equations. The new interpolation/interpolation functions are power-law functions of rupture time where rupture is predicted using the Wilshire equation [8-11]. The conventional and new approach are calibrated to the analytical Theta constants and creep deformation predictions compared. It is found that using Wilshire predicted rupture time with the new interpolation/extrapolation equation produces predictions that are on par with the original theta-projection method of prediction.

CHAPTER 6: CONCLUSIONS

discusses the conclusions made considering each study presented in this work followed by a proposition for future work. The conclusions drawn in each previous chapter are reviewed before a final conclusion is drawn on the validity of the modified theta-projection method compared to the original. It is concluded that the modified theta projection method provides an improved method of calibration and an interpolation/extrapolation function that is able to produce better

predictions under certain circumstances. Using the Wilshire method for rupture time prediction results in predictions of creep strain that are on par with those made using the traditional theta-projection method of rupture time prediction.

CHAPTER 2: BACKGROUND

2.1 INTRODUCTION

Understanding the mechanisms of the creep strain-time relationship is paramount to understanding how the theta projection model is able to predict deformation behavior in a material. In this chapter, a description of creep deformation and the stages or regimes that compose the duration of material service life are described. Next the theta-projection model and the process of calibration and prediction as proposed by Evans are described. Finally, the material used in this study, alloy P91, is discussed in detail.

2.2 CREEP DEFORMATION

Creep viscoplasticity, is the deformation of a material at a temperature-stress with time. This process of deformation occurs above and below the yield strength of a material [15-17]. The rate of creep deformation increases with temperature and stress. Deformation occurs in three distinct stages; primary, secondary, and tertiary creep [15-17]. The stages of creep deformation and the changes to each regime with respect to temperature and stress are illustrated in Figure 2.1: The transition through primary, secondary, and tertiary regimes of creep deformation.

.

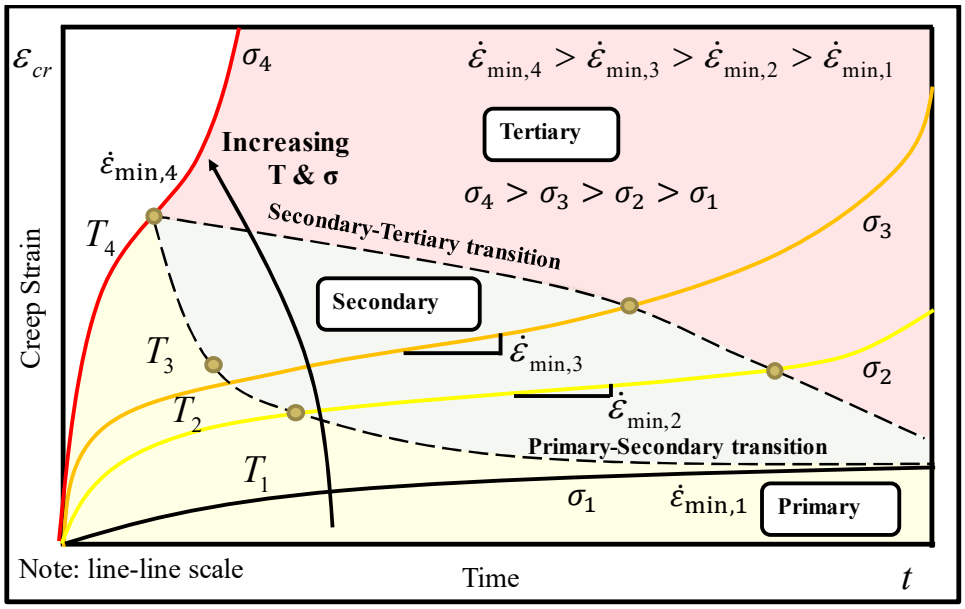

Figure 2.1: The transition through primary, secondary, and tertiary regimes of creep deformation.

Beginning with the primary regime, the strain in the material increases at an exponentially decaying rate until it enters the secondary regime whereby the rate of deformation becomes relatively constant. The behavior of the primary regime can be described mathematically using the time-hardening Norton-Bailey equation;

$$\varepsilon_c = A\sigma^n t^m \tag{1}$$

where A, n, and m are temperature-dependent and can be determined from uniaxial creep data [17]. The strain in creep resistant alloys such as Alloy P91 is small (less than 1% ductility) and often (for simplicity) neglected during prediction modeling. The primary regime gradually transitions to a steady-state increase in strain known as secondary creep. The behavior of the primary regime changes with temperature and stress, illustrated in Figure 2.1.

Secondary creep is transition between primary and tertiary creep regimes where strain-hardening and recovery mechanics are in balance create this quasi-steady-state regime. The minimum-creep-strain-rate is found within the secondary creep regime. As temperature and stress

increase, the. In extreme instances where temperature and stress are very high, the secondary regime will collapse to and the primary regime will transition directly into the tertiary regime.

Once in the tertiary creep regime, the strain in the material increases exponentially, often due to necking or cracks that propagated during loading in the material, until fracture. During the tertiary regime, a new concept is used to understand the rate of deformation; damage (ω), [17]. Though not utilized in the theta projection model, the tertiary regime is most proficiently modeled using damage. This is notable when comparing the effectiveness of the theta projection model to more comprehensive and in-depth models such as the sin-hyperbolic model which takes damage into account [3].

2.3 THE THETA-PROJECTION MODEL

The Theta-projection model was developed by R. W. Evans in 1985 in response to the limited predictive capability of older models such as the Norton-Bailey law [[*17*]. The theta-projection constitutive model relies on 4 material constants and is designed to mathematically fit all 3 regimes of the classical creep curve, at which it excels. The theta-projection equation is of the following form

$$\varepsilon = \theta_1(1-\exp(-\theta_2 t)) + \theta_3(\exp(\theta_4 t)-1) \tag{2}$$

where θ_1, θ_2, θ_3 and θ_4 are material constants measured in %-strain/hr. [4-7]. The equation is composed of two parts, the first a time-hardening equation governing the primary regime and the second a time-softening equation governing the tertiary regime, [Eqs.(3)&(4)] respectively.

$$\varepsilon_{pr} = \theta_1(1-\exp(-\theta_2 t)) \tag{3}$$

$$\varepsilon_{tr} = \theta_3(\exp(\theta_4 t)-1) \tag{4}$$

The relationship between [Eqs.(3)&(4)] and the classical creep curve shape is illustrated in Figure 3.2. Regarding the primary regime [Eq. (3)], θ_1 serves as the magnitude while θ_2 governs the exponential decay as creep transitions into the secondary regime. Likewise, in the tertiary regime [Eq. (4)], θ_3 serves as the magnitude while θ_4 governs the exponential acceleration of strain to fracture.

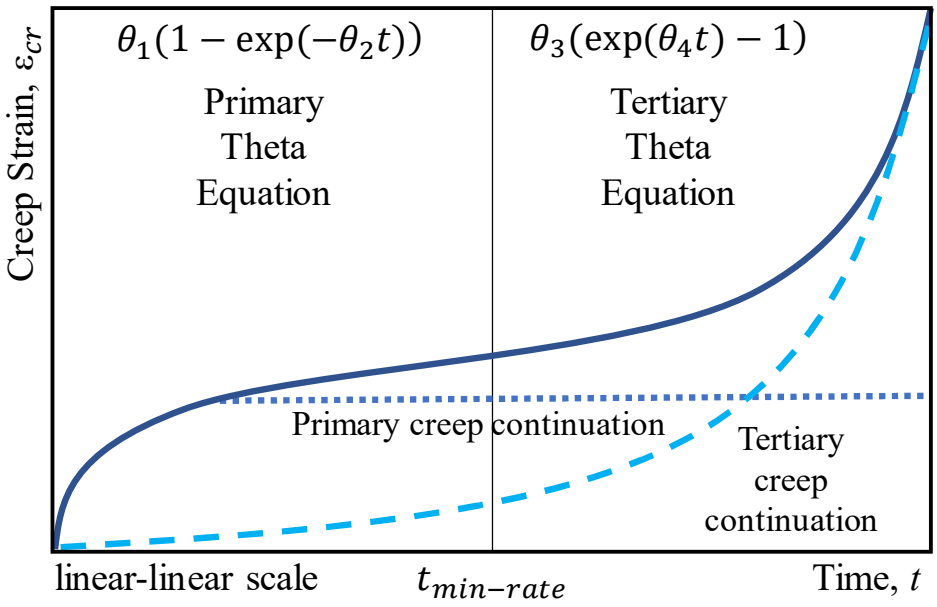

Figure 3.2: The theta projection model as it relates to the traditional creep curve.

Interpolation and Extrapolation

An interpolation/extrapolation function is used to relate θ_1, θ_2, θ_3 and θ_4 temperature and stress as follows

$$\ln(\theta_i) = a_i + b_i\sigma + c_iT + d_i\sigma T \tag{5}$$

where a_i, b_i, c_i and d_i are constants and $i = 1-4$ [4-7]. These interpolation/extrapolation equations [Eq.(5)] allow for predicted values of θ_1, θ_2, θ_3 and θ_4 to be determined for virtually

any temperature and stress condition. When plugging the predicted Thetas into [Eq.(2)], interpolated and extrapolated predictions of creep deformation can be made.

Evans developed a two-step process for applying the theta projection model; the first step involves calibrating the Theta constants by fitting [Eq. (2)] to individual creep deformation curves using a least square non-linear scheme [6,12]. The second step involves calibrating the interpolation/extrapolation functions using the calibrated Thetas and a weighted linear least square scheme [12,18]. Figure 4.3 illustrates the outcomes of calibration; the ability fit, interpolate and extrapolate**Error! Reference source not found.**. Evans concluded that the theta projection model excels at fitting creep deformation curves for several alloys including; 1CrMoV rotor steel, Ti.6.2.4.6, and the nickel-based superalloy IN-100, all above 700K, for a multitude of stresses [4,12,18,19].

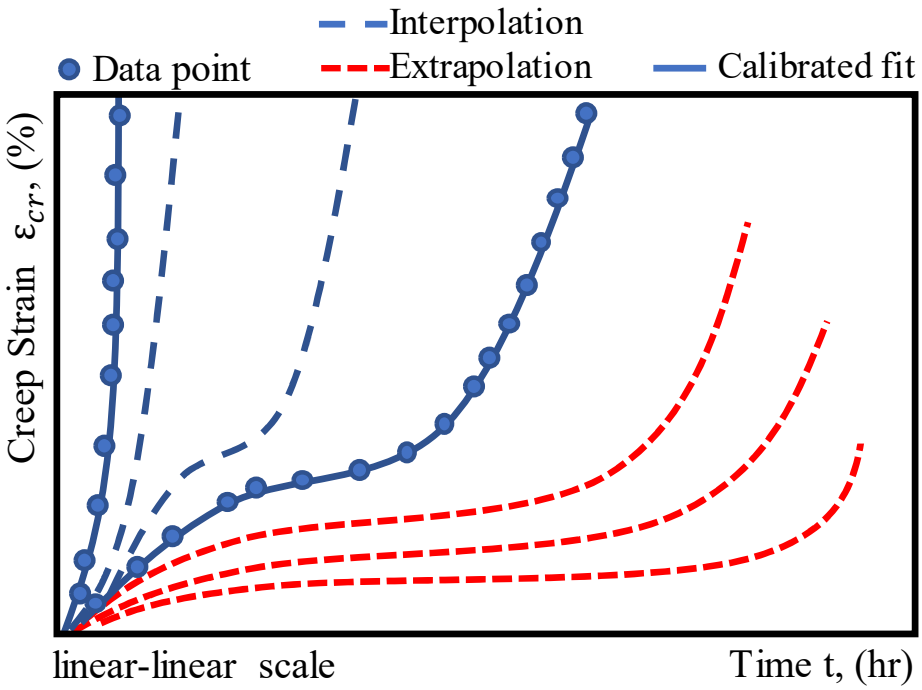

Figure 4.3: Sets of creep strain vs time test data with data interpolation and extrapolation.

Improvements and Modifications

Since inception, the theta projection model has been improved and modified in a number of ways. In a separate study conducted by Evans, he developed several improved interpolation/extrapolation equations after deeming [Eq.(5)] to be insufficient for long-term life prediction of 1CrMoV rotor steel [18]. The most effective equations are as follows

$$\ln(\theta_i) = a_i + b_i \frac{1}{T} + c_i \frac{\sigma}{T} \tag{6}$$

$$\ln(\theta_i) = a_i + b_i \frac{1}{T} + c_i \frac{\sigma}{T} + d_i \sigma \ln(\frac{1}{T}) \tag{7}$$

where [Eq.(6)] is superior if used with un-weighted least squares and [Eq.(7)] is superior if used with weighted least squares. The weight function is as follows

$$W_i = \frac{\theta_i^2}{Var[\theta_i]} \tag{8}$$

where $Var[\theta_i]$ is the variance related to the predicted value of θ_i [18,20].

The most significant innovation of the theta projection model by Evans was the development of a 6-Theta-projection model [19]. The functional form of the 6-theta-projection model is as follows;

$$\varepsilon = \theta_1(1-\exp(-\theta_2 t)) + \theta_3(\exp(\theta_4 t)-1) + \theta_5(1-\exp(-\theta_6 t)) \tag{9}$$

where θ_5 and θ_6 serve to better fit the early primary regime. The interpolation/extrapolation equation is essentially the same as [Eq.(5)] though now $i = 1-6$. It was found that the original 4-Theta-projection model was not able to predict the primary regime at times to low strains accurately. To overcome this limitation, the 6-Theta-projection model introduces an additional hardening function with two material constants, θ_5 and θ_6, to better fit the early stages of primary creep strain [19,21]. Evans concluded that the 6-Theta-projection model produced superior long-

term failure and low primary creep predictions at low strains compared to the 4-Theta-projection model when applied to 1CrMoV rotor steel test data [19,21]. The results are similar when applied to 2419-T851 aluminum alloy [22]. It is evident that the 6-Theta-projection model outperforms the 4-Theta-projection model for different materials. The current study focuses on the original 4-Theta-projection model. The 6-Theta-projection model allows for further improvement and future work.

2.4 MATERIAL: ALLOY P91

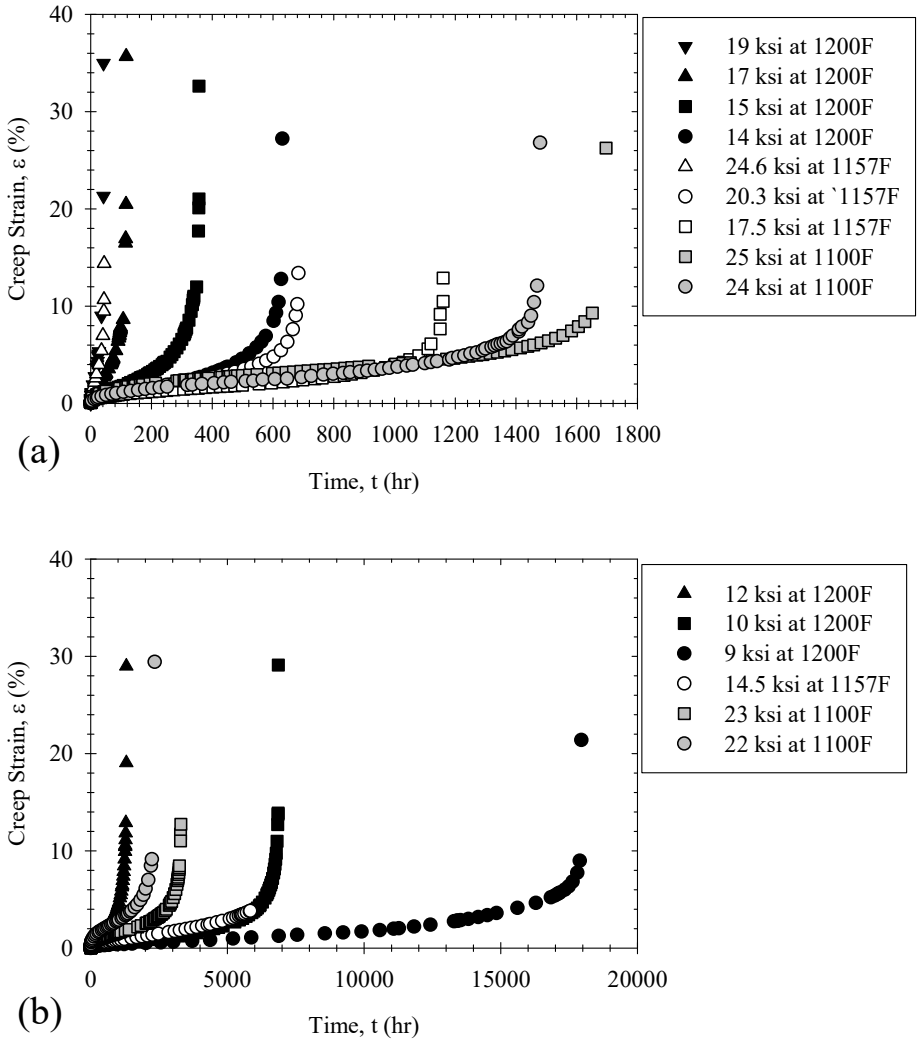

Figure 5.4: Creep deformation curves of Alloy P91 at (a) short- and (b) intermediate- duration across 1200, 1157, and 1100°F.

Creep strength enhanced ferric (CSEF) steels were developed in to combat the effects of creep on components used in power plants that are subject to high-temperatures and high-stress, such as boilers, stream tubes, and turbine blades [[*23*-[*26*]. Due to their lower coefficient of thermal expansion than austenitic steels, CSEF steels are more suited to dealing with high-temperature conditions. Introduced in the 1960's, CSEF utilize a chromium content of 12% to ensure good creep resistance, high corrosion and wear resistance, and hardenability. It was found that the high amount of chromium caused early failure of components due to unexpected precipitation [23-[*26*]. Later research by Oak Ridge National Laboratory demonstrated the improvement in creep strength in the material by lowering the chromium (Cr) percentage from 12% to 9% [[*23*]. Lowering the Cr also avoids the formation of δ-ferrite, which is detrimental to the alloy. For this purpose and to increase strength and hardness of the alloy, 1% molybdenum (Mo) is used to solid solution strengthen the material. vanadium (V) is used to aid in the formation of carbide precipitates which enhances the corrosion strength [[*23*-[*26*]. This element combination forms 9Cr-1Mo-V or P91 alloy steel.

The test data used in this work was collected by Oak Ridge National Laboratory [[*14*]. It consists of sets of creep deformation data collected at various isostresses at 3 distinct isotherms; 1200ºF, 1157ºF and 1100ºF. Data at all 3 isotherms are used in the assessment of the theta-projection model. Only data at 1200ºF is used to assess the analytical method of calibration and the modified interpolation/extrapolation method. The sets of test data are illustrated in Figure 5.4.

CHAPTER 3: THETA-PROJECTION PERFORMANCE REVIEW

3.1 INTRODUCTION

Overview

The objective of this study is to demonstrate the performance of Theta-projection using the conventional calibration approach and interpolation/extrapolation functions. To accomplish this objective; a systematic method of fitting and prediction is applied. A numerical optimization algorithm is written in the MATLAB programming language. Using the algorithm, the theta projection model is calibrated to creep deformation test data of alloy P91. The data consists of deformation curves recorded from tests conducted at increasing stresses at 3 different temperatures; 1100, 1157 and 1200°F. The calibrated theta material constants are then fit to simplified interpolation functions of temperature and stress. Predictions are made using the calibrated constants. A qualitative assessment is performed using creep deformation plots to compare the calibrated and interpolated fits to the experimental data. A quantitative assessment is performed using NMSE tables to compare the error between calibrated and interpolated fits.

3.2 CALIBRATION AND FUNCTIONALIZATION

Calibration Algorithm

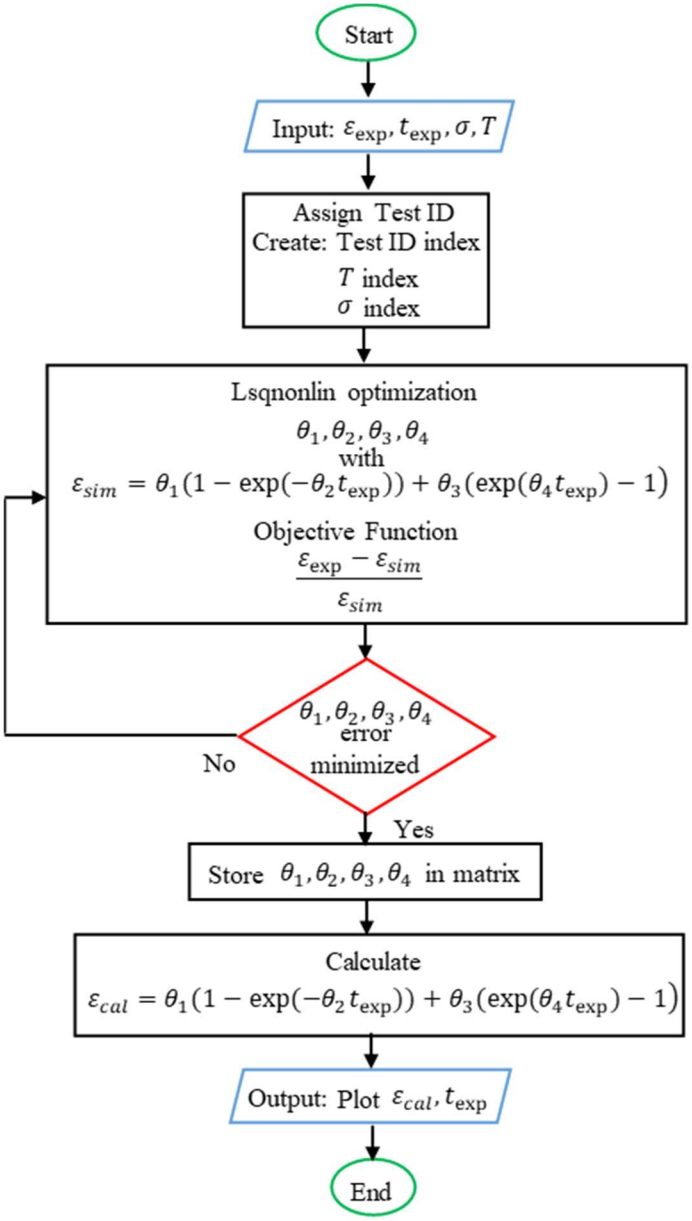

Figure 6.1: MATLAB algorithm for calibration of creep deformation data using the theta projection model.

A MATLAB calibration algorithm has been developed to calibrate the Theta constants to creep deformation data, in Figure 6.1. This algorithm coincides with the two-step process defined by Evans and detailed in CHAPTER 2: BACKGROUND

[**Error! Reference source not found.**]. In this study, a non-linear least-square scheme is to calibrate the theta constants [**Error! Reference source not found.**,**Error! Reference source not found.**] using an objective function to minimize error. The objective function is as follows

$$error = \frac{\varepsilon_{\exp,i} - \varepsilon_{sim,i}}{\varepsilon_{sim,i}} \tag{10}$$

where $\varepsilon_{\exp,i}$ is the experimental strain from the test data and $\varepsilon_{sim,i}$ is the strain of the calibrated fit generated by the algorithm. The least-square non-linear scheme attempts to minimize the sum of the objective function squared for all data points considered. The equation is

$$\min_x \left\| f(x) \right\|_2^2 = \min_x \left(f_1(x)^2 + f_2(x)^2 + \ldots + f_n(x)^2 \right) \tag{11}$$

where $f(x)$ is the error function [Eq.(10)]. The least-square non-linear scheme with respect to the error function serves as a variant of the normalized mean square error (NMSE). The constants θ_1, θ_2, θ_3 and θ_4 are constrained to a lower bound of zero and an upper bound of ten.

Theta Constant Calibration

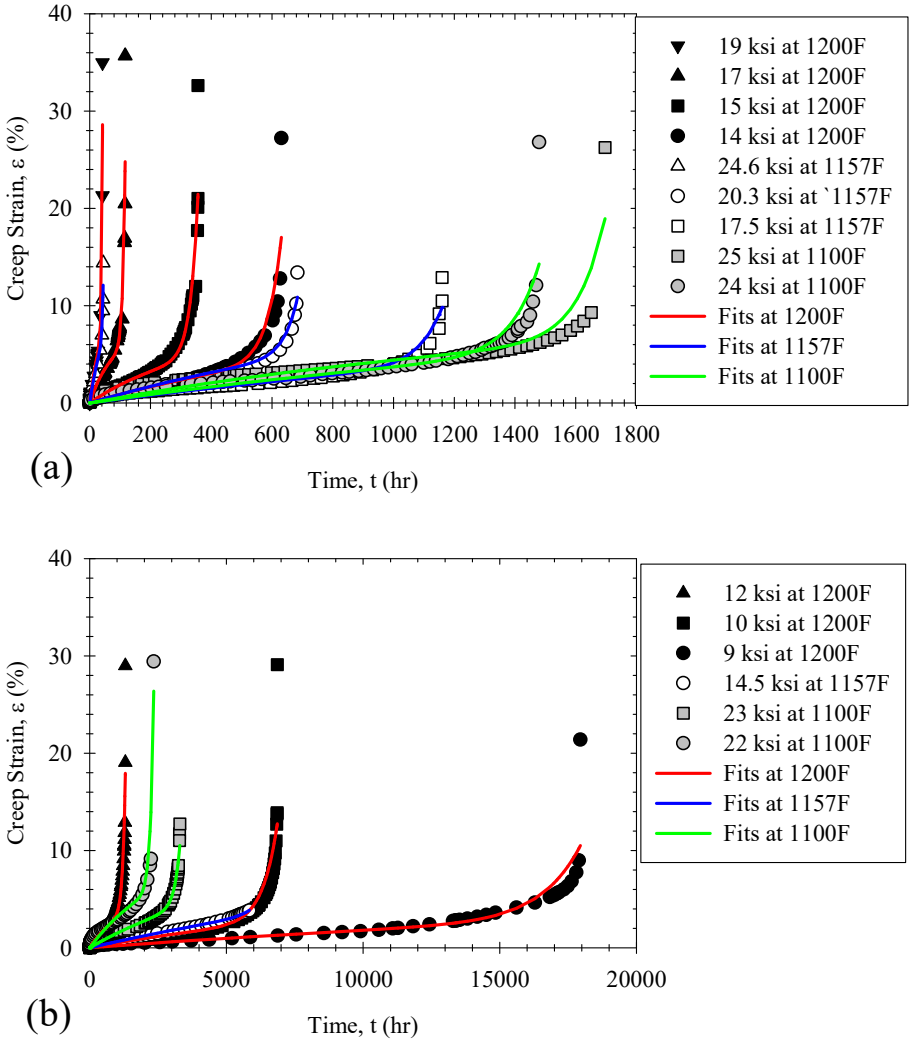

Figure 7.2: Fits to creep deformation curves (a) short- and (b) intermediate- duration across 1200, 1157, and 1100°F using calibrated theta constants.

The MATLAB calibration algorithm was applied to determine the Theta constants for Alloy P91. The creep data for Alloy P91 is available in section 2.4 of chCHAPTER 2: BACKGROUND

. Creep deformation predictions using the calibrated Theta constants match the experimental data well, as illustrated in Figure 7.2. All fits exhibiting a NMSE of less than one (Table 1). Due to the physical limitations of the model, the fits do not accurately depict the full ductility of the specimens. Rather, they depict a conservative representation of creep strain near rupture time. The predicted creep ductility decreases as stress decreases at 1200 and 1157˚F, similar to the experimental data. At 1100^0F, the predicted creep ductility increases as stress decreases which does not match the experimental data. Despite the differences in ductility, the qualitative comparison of Figure 7.3, and the low NMSE correspond with Evans's conclusion that the theta-projection model excels at fitting creep deformation. The NMSE equation is as follows

$$NMSE = \frac{1}{n}\sum_{i=1}^{n}[(X_{sim,i} - X_{\exp,i}) / X_{\exp,i}]^2 \tag{12}$$

where n is the number of data points and X is the simulated or experimental data denoted by subscript.

Table 1 – NMSE values of calibrated fits and interpolated fits relative to experimental data for stresses at each isotherm.

Temperature T, (°F)	Stress σ, (ksi)	Calibrated prediction NMSE	Interpolated prediction NMSE
1200°F	19.0	0.2667	10187.0
	17.0	0.2547	0.25610
	15.0	0.2234	0.46410
	14.0	0.1659	0.15930
	12.0	0.1344	0.14590
	10.0	0.1323	0.15570
	9.00	0.2119	27.8394

1157°F	24.6	0.9833	0.31230
	20.3	0.7538	947680
	17.5	0.5003	0.36180
	14.5	0.2684	0.27820
1100°F	25.0	0.2733	0.33210
	24.0	0.1750	0.23280
	23.0	0.2362	531853
	22.0	0.3557	0.43270

The physical limitation of Theta projection arises from the functional form. While the primary and tertiary creep portions of the theta projection model are accurate, the secondary creep regime (interface between the two functions) exists mathematically as a point.

$$\dot{\varepsilon}_{\min} = f(t_{\min}) \tag{13}$$

In experimental data, the secondary regime exists as a range and encompasses most of the creep deformation curve. During optimization, the equally weighted objective function leads to accuracy in the secondary creep regime at the expense of the tertiary creep regime. Despite the under-prediction of creep ductility, the calibrated model fits the primary and secondary regimes well for creep strain below 5%.

Material Constant Dependencies

Analyzing each isotherm separately, the interpolation functions relating each theta constant to temperature and stress become solely dependent on stress. This strictly stress dependency effectively regresses [Eqs.(5)-(7)] to a linear function when temperature is held constant;

$$\ln(\theta_i) = (c_i + d_i T)\sigma + (a_i + b_i T) \tag{14}$$

when relating to [Eq. (5)] and

$$\ln(\theta_i) = (c_i \frac{1}{T})\sigma + (a_i + b_i \frac{1}{T} + d_i \ln \frac{1}{T}) \quad (15)$$

when relating to [Eqs.(6)&(7)] where in each equation the first term is the slope and the second term the intercept on a logarithmic scale. In this study, the isotherm are analyzed individually such that the linear interpolation functions [Eqs.(14)&(15)] can be employed. The interpolation function used in this study corresponds to [Eq. (14)], slope and intercept data is presented in Table 2.

Table 2 – Slope and intercept trend information for each calibrated theta constant per isotherm for [Eq.(14)]

	1200ºF		1157ºF		1100ºF	
	Slope $c_i + d_i T$	Intercept $a_i + b_i T$	Slope $c_i + d_i T$	Intercept $a_i + b_i T$	Slope $c_i + d_i T$	Intercept $a_i + b_i T$
θ_1	0.061	1.018	0.001	2.251	0.008	2.085
θ_2	0.649	-15.54	0.558	-17.75	0.220	-13.08
θ_3	-0.205	-8.338	0.137	-14.96	0.455	-26.06
θ_4	0.607	-12.36	0.470	-12.94	0.146	-8.214

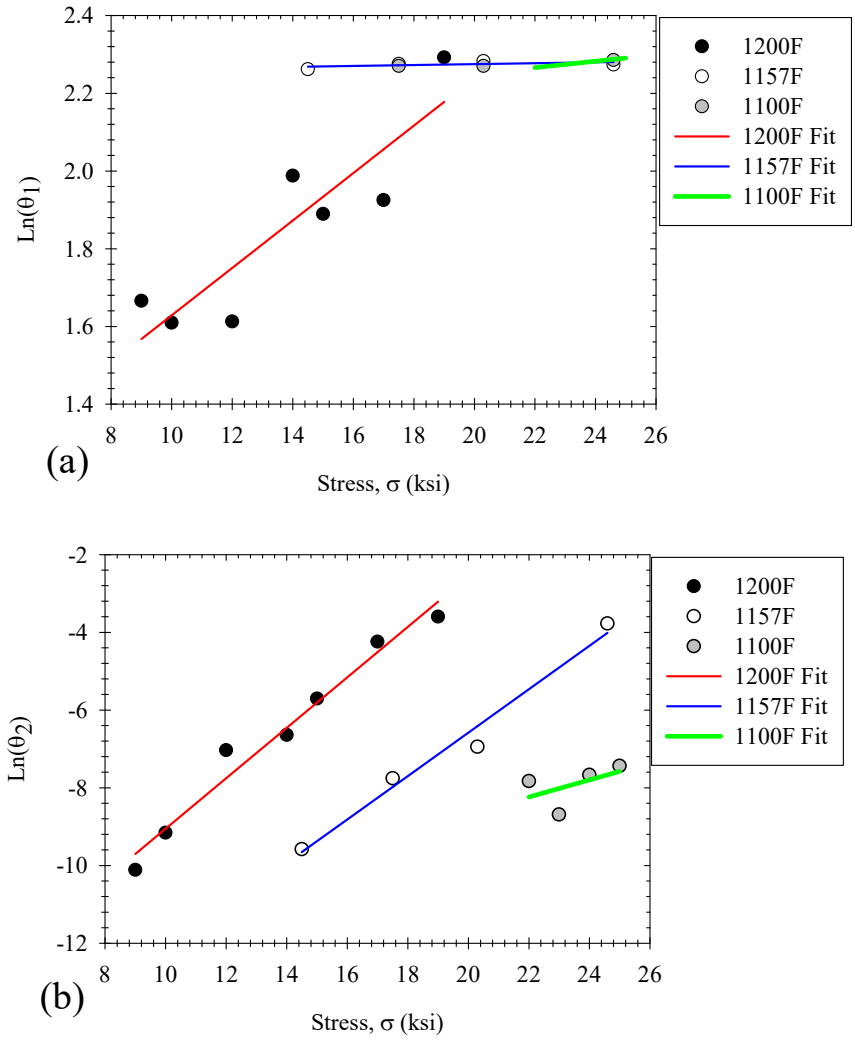

Figure 8.3: Fits of [Eq.(14)] through calibrated (a) - θ_1 , (b) - θ_2 values at 1200, 1157 and 1100 ℉.

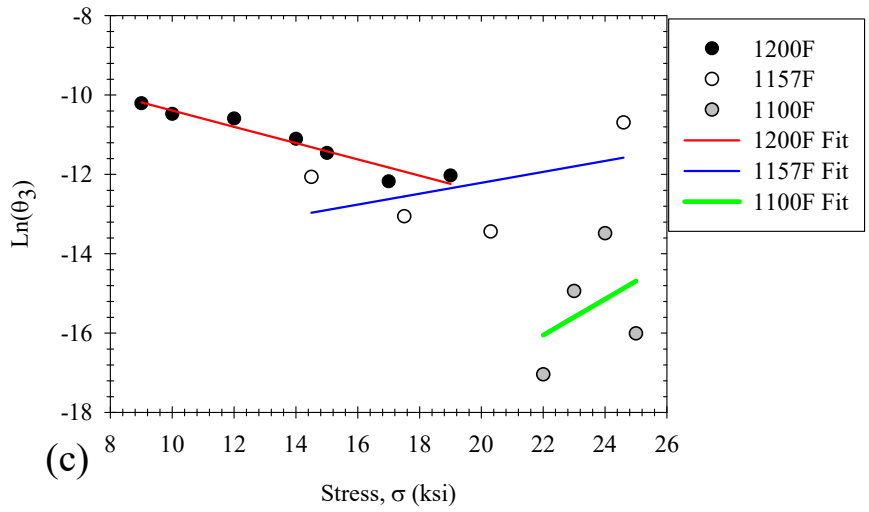

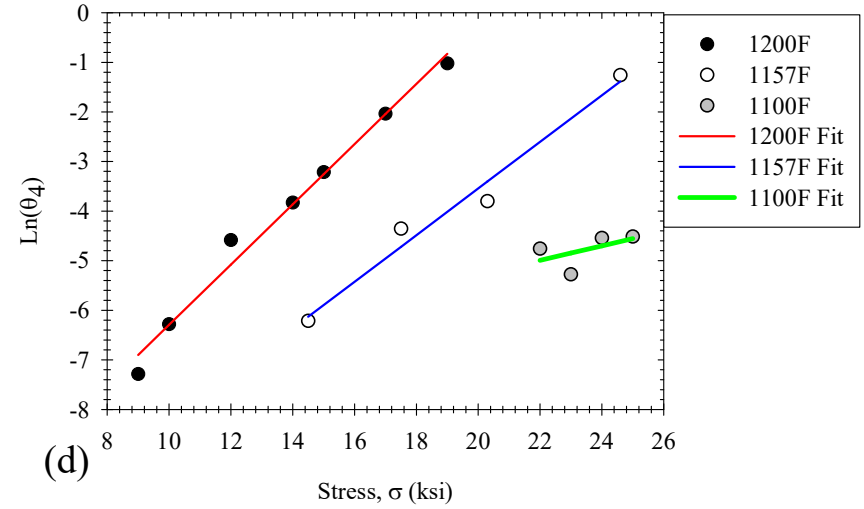

Figure 9.4: : Fits of [Eq.(14)] through calibrated (c) - θ_3 and (d) - θ_4 values at 1200, 1157 and 1100 ℉.

3.3 RESULTS

Evaluation of Material Constants

The calibrated theta constants are plotted with respect to stress per isotherm as illustrated in Figure 8.3. The data points represent the calibrated Theta constants. The lines represent the fit of the interpolation/extrapolation functions [Eq. (14)] to the calibrated Theta constants. The slopes of the interpolation/extrapolation functions for θ_2 and θ_4 exhibit a consistent linear trend across

all isotherms, decreasing as temperature decreases. The slopes of the interpolation functions for θ_1 and θ_3 are inconsistent.

The interpolation/extrapolation fits of the θ_1 constants are plotted with respect to stress per isotherm in Figure 8.3 Figure 9.4. When applying numerical optimization, the calibrated constants are not necessary associated with the physical stages of creep. Consequentially, the slopes of the θ_1 interpolation functions for each isotherm do not present a consistent trend, seen in Table 2. Theta 1 does not exhibit a consistent trend with stress at 1200ºF. It does however exhibit a trend at 1157 and 1100ºF. The slope of the interpolation/extrapolation function remains constant across all isotherms but dramatically increases within a short interval of temperature approaching zero.

The interpolation/extrapolation fits of the θ_2 constants are plotted with respect to stress per isotherm in Figure 8.3. The θ_2 constants exhibit the most consistent interpolation function trend across all 3 isotherms. The slope of the interpolation/extrapolation function decreases with temperature.

The interpolation/extrapolation fits of the θ_3 constants are plotted with respect to stress per isotherm in Figure 9.4. The constant θ_3 is the most inconsistent Theta constant observed. Numerical optimization prevents the isolation of a single regime and is the cause of this inconsistency. Moving from high to low temperature, the slope of the interpolation/extrapolation function goes from negative, to positive, to decreasing positive. The quality of calibration also decreases with temperature where the interpolation/extrapolation predictions do not match the calibrated theta constants.

The interpolation/extrapolation fits of the θ_4 constants are plotted with respect to stress per isotherm in Figure 8.3 Figure 9.4. The constant θ_4 is similar in behavior to θ_2. The

interpolation/extrapolation functions match the calibrated θ_4 exhibiting low scatter. As temperature decreases, the slope of the interpolation/extrapolation function approaches zero. The θ_4 slopes decrease at a faster rate than the θ_2 constants.

While the interpolation function trends in the slopes of θ_2 and θ_4 behave as expected, the slope trends of θ_1 and θ_3 deviate from what Evans has shown [[*18*]. The major deviation from the expected behavior is reflected in the calibrated values of θ_3. As stress increases, Evans has shown that the calibrated values of θ_3 should strictly decrease [[*18*]. This is true for the 1200ºF isotherm, however for the 1157 and 1100ºF isotherms, θ_3 calibrated values tend to increase as stress increases. This can be reconciled in the fact that there exists a significant amount of scatter in calibrated θ_3 values for temperatures similar to 1100ºF [[*18*]. This may be the result of the difference in material as the study of reference conducted by Evans utilized 1Cr-Mo-V rotor steel while this study focuses on alloy P91 9Cr-1Mo-V [[*18*]. The similarities in the calibrated and interpolated trends found in this study and those found by Evans lends validity to the claim that these theta predictions are reasonable. In summary; the calibrated constants θ_2 and θ_4 consistently present a trend of decreasing slopes in the interpolation functions, which coincides with work done by Evans, while calibrated values of θ_1 and θ_3 do not [[*18*].

Predictions using Interpolation/Extrapolation Functions

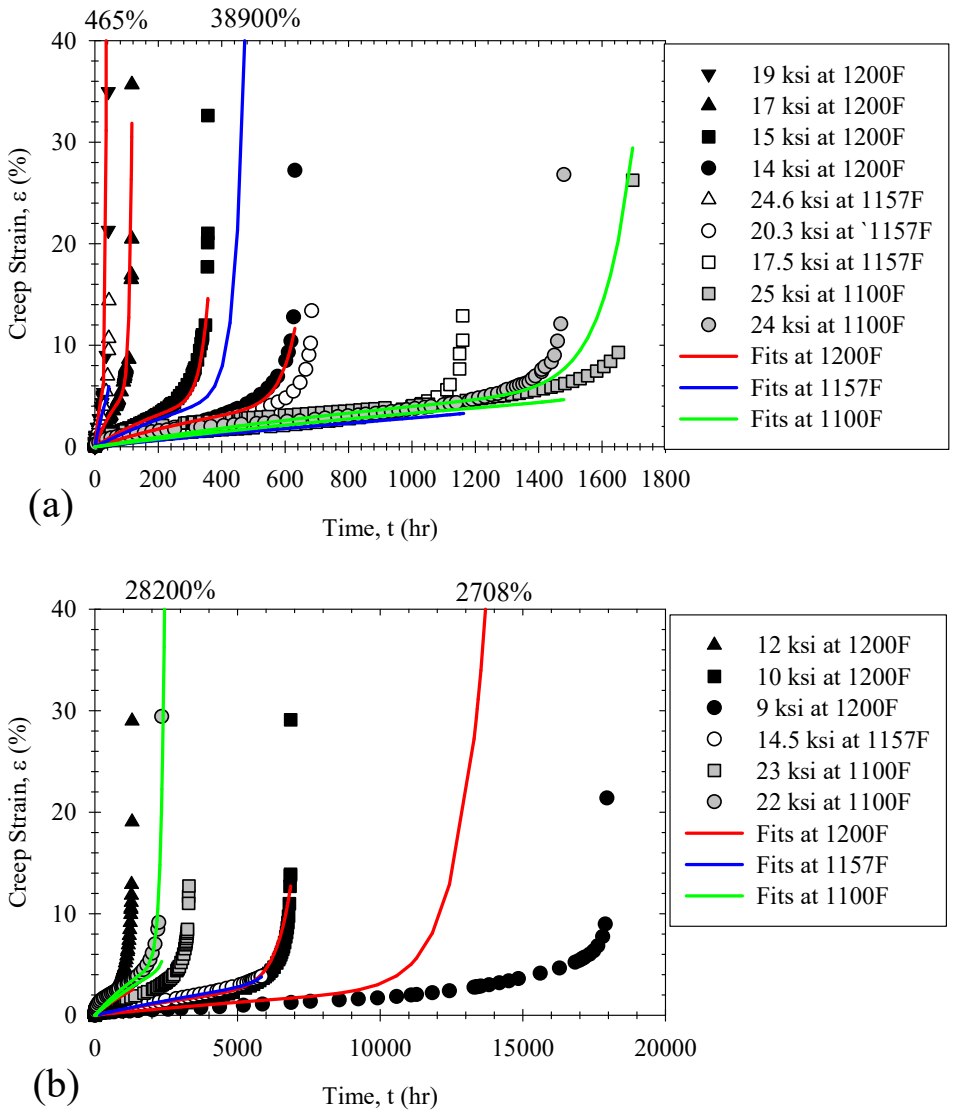

Figure 10.5: Interpolated predictions of creep deformation curves compared to experimental data at (a) short- and (b) intermediate- duration across 1200, 1157, and 1100°F.

Now that the interpolation/extrapolation functions [Eq.(14)] have been fit to the calibrated Theta constants, given a desired stress and temperature condition, the appropriate Theta constants can be calculated and creep deformation predictions generated [Eq.(2)]. To evaluate the quality of

predictions, the known creep deformation curves are predicted using the interpolation/extrapolation functions [Eq.(14)] as illustrated in Figure 10.5. To distinguish between the different predictions made, those featured in Figure 7.2 will be referred to as calibrated theta constant predictions while those conducted using interpolated theta constants featured in Figure 10.5 will be referred to as interpolations.

The predictions using calibrated theta constants, having minimal error relative to the test data, serve as references to optimal creep behavior. This error is illustrated in Table 1. The error of the predictions made using interpolated theta constants to the experimental data ranges from minimal to drastic. This is in part to the sensitivity of the model to minute shifts in theta constants. The interpolation function fits of θ_1, θ_2, θ_3 and θ_4 across all three isotherms depicted in Figure 8Figure 9.4 allow for a generalized prediction when of theta constants at their respective conditions of temperature and stress, consequentially the predictions made using interpolated theta constants will not be as accurate to the experimental data as the calibrated fits. The error shown between the predictions made using interpolated theta constants and the experimental data in Table 1 can be reconciled when the differences between creep curves at identical conditions are considered.

The nature of creep deformation is such that it can be very unpredictable, with multiple curves recorded at identical conditions of temperature and stress behaving radically different from one another. For the most part, the interpolated predictions of Figure 10.5 represent unpredictability. There are 4 interpolations where the error between the fits and the experimental data is incredibly large. At 1200ºF, the interpolations at 9 and 19 ksi dramatically over predicts creep strain ending in a final 465% and 2708% strain respectively. At 1157ºF, the interpolation at 20.3 ksi over predicts strain as well, predicting a rupture strain of 38900% strain. Finally, at the 1100ºF isotherm, the fit of 23 ksi predicts a final strain of 28200%. These incredibly high strain

predictions are due to the sensitivity of the Theta-projection model to the previously discussed shifts in Theta constants given by the interpolation function fits of θ_1, θ_2, θ_3 and θ_4 across all three isotherms in Figure 8Figure 9.4.

3.4 CONCLUSIONS

The numerical optimization process yields excellent predictions made using calibrated theta constants relative to the experimental data. When interpolation/extrapolation functions are applied the inconsistent trends in the Theta constants with respect to stress and temperature result in grossly inaccurate predictions There is a need to identify theta constants that fit the creep deformation data but also exhibit a more consistent trend with stress and temperature. This would result in more accurate interpolations. A modified approach to calibration may result in improved theta constant trends with stress and temperature.

The drastic shift in calibrated theta constants across all isotherms is evidence that numerical optimization does not associate the constants with the physical stages of creep. When constrained to minimal error, the algorithm was only able to calibrate theta constants that lacked the uniformity needed for accurate prediction.

CHAPTER 4: ANALYTICAL CALIBRATION TECHNIQUE

4.1 INTRODUCTION

In the previous chapter, it was discovered that applying the theta-projection model using numerical optimization and the standard interpolation/extrapolation functions results in poor predictions of creep deformation. The current chapter, an analytical approach to calibration is introduced and compared to numerical optimization.

The use of an analytical approach to calibration of the theta-projection model in the place of or in tandem with numerical optimization may improve the ability of the model to predict creep deformation. What is meant by an analytical approach is a method to give physical meaning to θ_1, θ_2, θ_3 and θ_4 relative to individual sets of experimental data. This is possible by building on the work begun by Evans in separating the theta-projection model [Eq.(2)] by creep regime, then relating to θ_1, θ_2, θ_3 and θ_4 to the parts of their respective regime that they are meant to describe. Relating each constant to the data individually and independently ensures a more realistic trend in to θ_1, θ_2, θ_3 and θ_4 as stress and temperature change the behavior of the data.

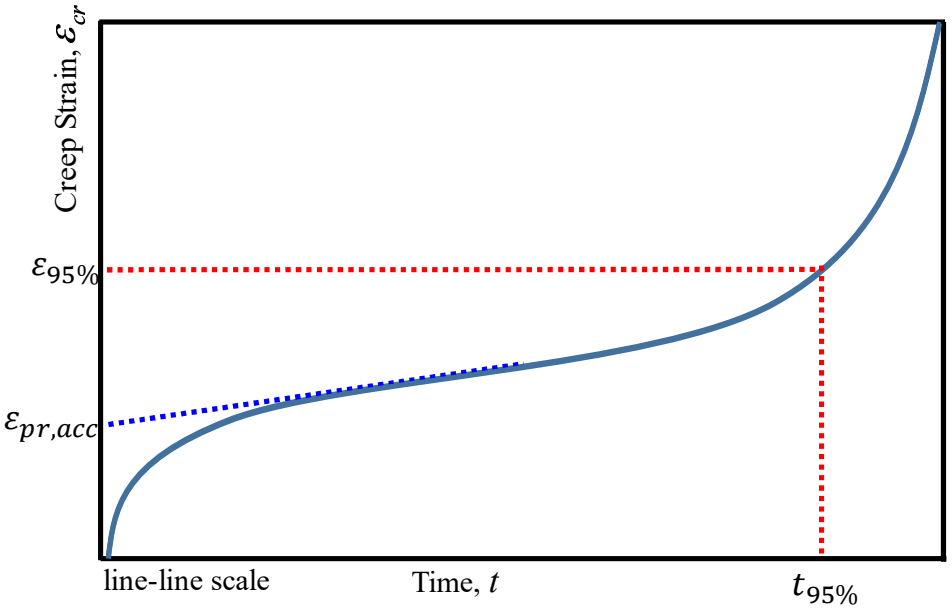

Figure 11.1: Key areas of creep deformation behavior as they relate to the analytical calibration equations.

4.2 ANALYTICAL APPROACH TO CALIBRATION

The theta material constants can be analytically derived from experimental data in the following manner. When $t \to \infty$, [Eq.(3)] hardens to a fixed value of primary strain

$$\varepsilon_{pr,a} = \theta_1 \tag{16}$$

where the material constant θ_1 is equal to $\varepsilon_{pr,a}$ the acccumulated primary creep strain. The $\varepsilon_{pr,a}$ is obtained from experimental data by plotting $\dot{\varepsilon}_{\min}$ as a line on the creep deformation curve (illustrated in Figure 11.1) and adjusting the y-intercept so that the $\dot{\varepsilon}_{\min}$ line matches the secondary creep regime of the data.

Considering the primary theta-projection model, replacing θ_1 with the value of the intersection, θ_2 can be identified

$$\theta_2 = -\frac{1}{t_{pr,sub}} \ln\left(1 - \frac{\varepsilon_{pr,sub}}{\theta_1}\right) \tag{17}$$

where $\varepsilon_{pr,sub}$ is just below the primary strain, with corresponding time $t_{pr,sub}$.

When $t \to \infty$, [Eq.(3)] hardens to a fixed value of primary strain and subsequently the theta projection model [Eq.(2)] simplifies to

$$\varepsilon_f = \theta_1 + \theta_3(\exp(\theta_4 t) - 1) \tag{18}$$

where ε_f is creep ductility and t_f is the rupture time. Rearranging [Eq.()] for θ_3 as a function of θ_1 and θ_4 gives

$$\theta_3 = \frac{\varepsilon_{cr} - \theta_1}{\exp(\theta_4 t_f) - 1} \tag{19}$$

The material constants θ_3 and θ_4 represent two unknowns, an additional equation is needed to solve. Taking the first and second derivatives of [Eq.(4)] yields

$$\dot{\varepsilon}_{cr} = \theta_3 \theta_4 \exp(\theta_4 t_f) \tag{20}$$

and

$$\ddot{\varepsilon}_{cr} = \theta_3 \theta_4^2 \exp(\theta_4 t_f) \tag{21}$$

respectively. Since creep ductility is invariant at a set isostress and isotherm, the final creep strain rate and acceleration at rupture are also invariant. Algebraically manipulating [Eq.(20)&(21)] furnishes material constant θ_4 as follows;

$$\theta_4 = \frac{\ddot{\varepsilon}_{cr}}{\dot{\varepsilon}_{cr}} \tag{22}$$

where final creep strain rate, $\dot{\varepsilon}_f$, and final creep strain acceleration, $\ddot{\varepsilon}_f$, are obtained from experimental data. Substituting, θ_4 from [Eq.(22)] into [Eq.(19)] furnishes material constant θ_3.

4.3 CALIBRATION DATA

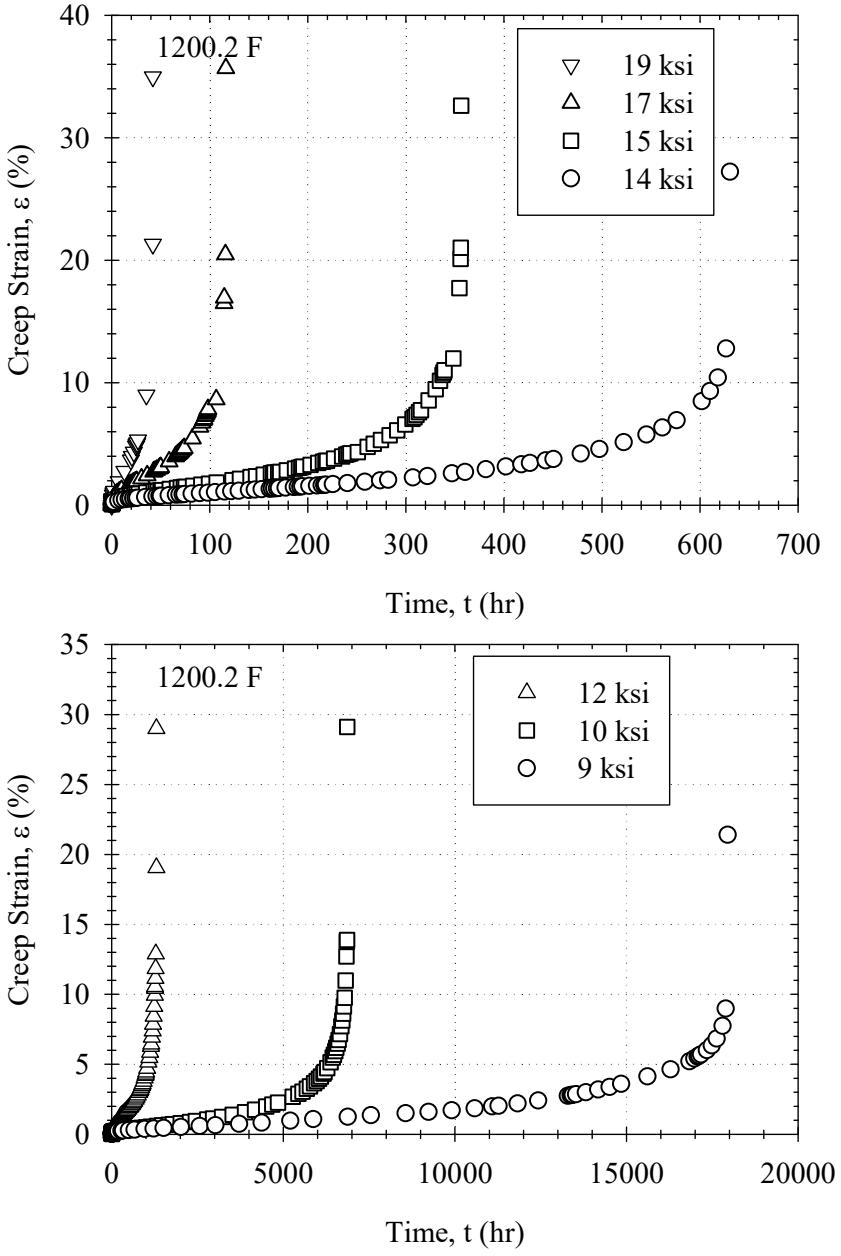

Figure 12.2: Data used in calibration, taken from tests conducted at 19, 17, 15, 14, 12, 10, and 9 ksi at 1200^{0}F.

In completing this analysis, the calibration data from CHAPTER 3: THETA-PROJECTION PERFORMANCE REVIEW

at 1200ºF is used, illustrated in Figure 12.2. This calibration data is composed of 7 sets of full creep deformation tests conducted at 19, 17, 15, 14, 12, 10 and 9 ksi all at the aforementioned

isotherm. This data is also used as validation data to compare the numerical and analytical optimization approaches.

4.4 NUMERICAL OPTIMIZATION RESULTS

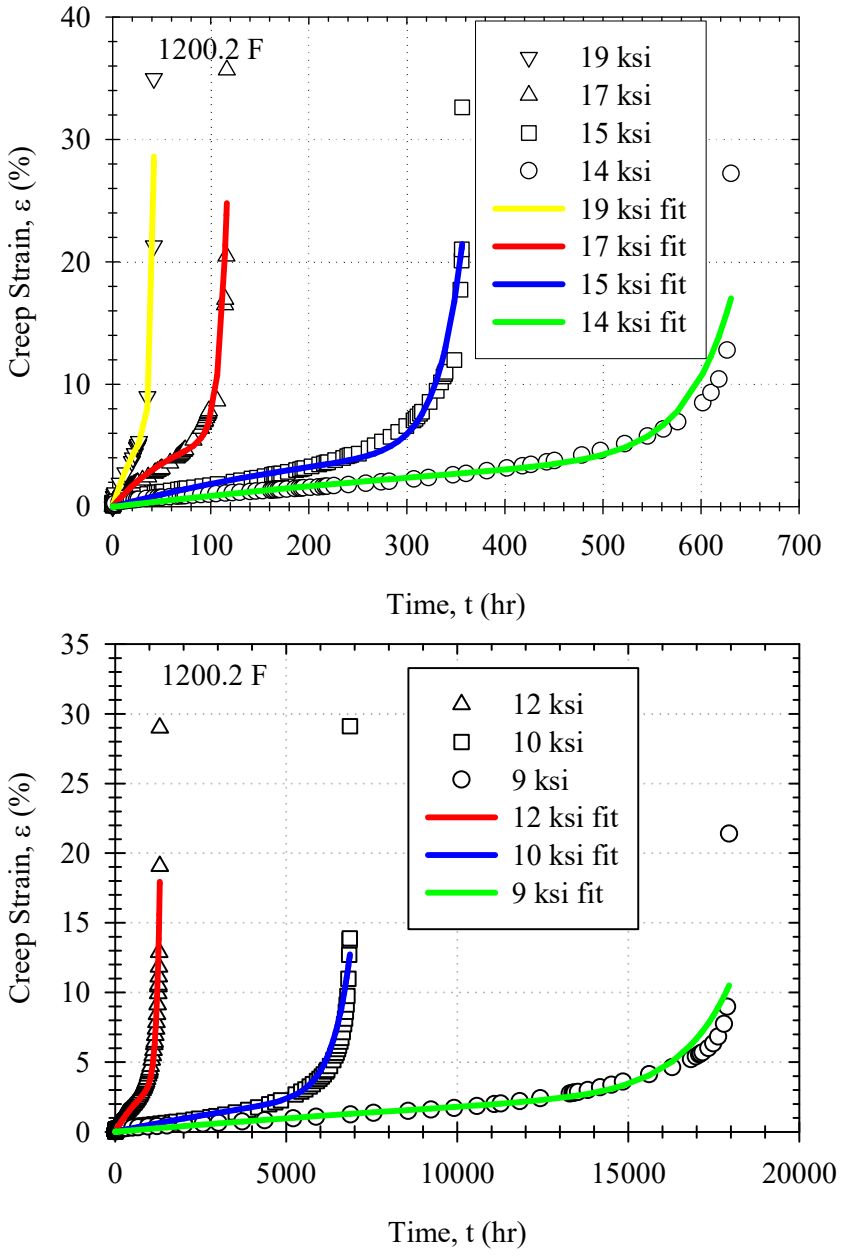

Figure 13.3: Calibrated fits to test data using a least-square non-linear numerical optimization scheme.

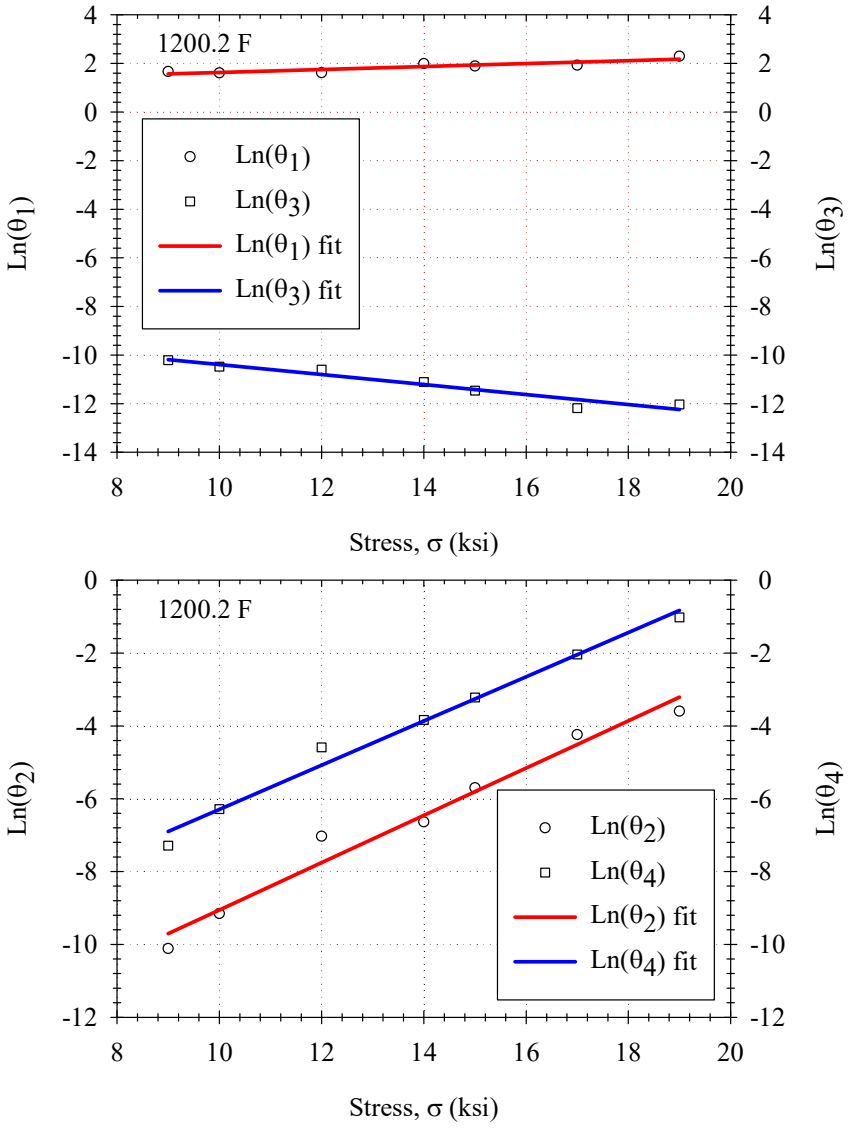

Figure 14.4: Theta constants calibrated using a least-square non-linear numerical optimization scheme.

Calibrating the theta-projection model to the calibration data using numerical optimization produces excellent fits to the data. The NMSE is presented in Table 3. Using [Eq.(14)], values of θ_1, θ_2, θ_3 and θ_4 are predicted for 19, 17, 15, 14, 12, 10, and 9 ksi at 1200ºF. The natural logarithm of calibrated and predicted theta constants is plotted against stress and compared in Figure 14.4. The predicted theta constants appear as a fit line through the calibrated constants, representing accurate prediction, however when used to generate creep deformation predictions, the results vary drastically from validation data.

Theta constants from Figure 14.4 are used to generate creep strain predictions at the same conditions as calibration data. These predictions are compared to said calibration data in Figure 15.5. Using these predicted theta values, the quality of the resulting predictions varies drastically. The predictions made at 17, 15, 14 and 12 ksi are reasonable, they depict accurate rupture ductility and the behavior of the primary, secondary and tertiary regimes behaves similar to the calibration data. The behavior of predictions made at 19, 12 and 9 ksi, however, differ drastically from calibration data at 469, 2, and 2687% creep ductility respectively. The difference in error between the calibrated fits and predicted creep deformation curves is presented in Table 3.

It is evident that though the original method of calibration for the theta-projection model may result in reasonable predictions for some tests, not all are accurate enough to be considered practicable. This is due to the nature of numerical optimization discussed in CHAPTER 3: THETA-PROJECTION PERFORMANCE REVIEW. Numerical optimization produces values of θ_1, θ_2, θ_3 and θ_4 that have no relevance to one another across isotherms. This lack of a trend in theta constants results in sporadic functionalization with [Eq.(14)]. This results in predicted theta constants that are not compatible with one another and in turn causes erratic behavior of creep deformation predictions. It is evident that establishing a realistic trend in theta constants from isostress to isostress is necessary for good prediction.

The Theta values that result from prediction using numerical optimization are illustrated in Table 3. The NMSE of the predictions made using the theta values in Appendix Table 1 are presented in Table 3. These values are presented for comparison with those resulting from calibration using the analytical technique. Examining Appendix Table 1, it is evident that values of θ_1, θ_2, θ_3 and θ_4 do not maintain a consistent trend as stress decreases. The most scatter in theta constants is present in θ_1 and θ_3. This lack of a trend causes an incompatible combination of θ_1, θ_2, θ_3 and θ_4, resulting in poor prediction.

Table 3 – Normalized mean square error comparison of calibrated fits and predictions made using numerical optimization.

Isostress	Calibration NMSE	Prediction NMSE
19 ksi	0.2119	27.839
17 ksi	0.1323	0.1557
15 ksi	0.1344	0.1459
14 ksi	0.1659	0.1593
12 ksi	0.2234	0.4641
10 ksi	0.2547	0.2561
9 ksi	0.2667	10187

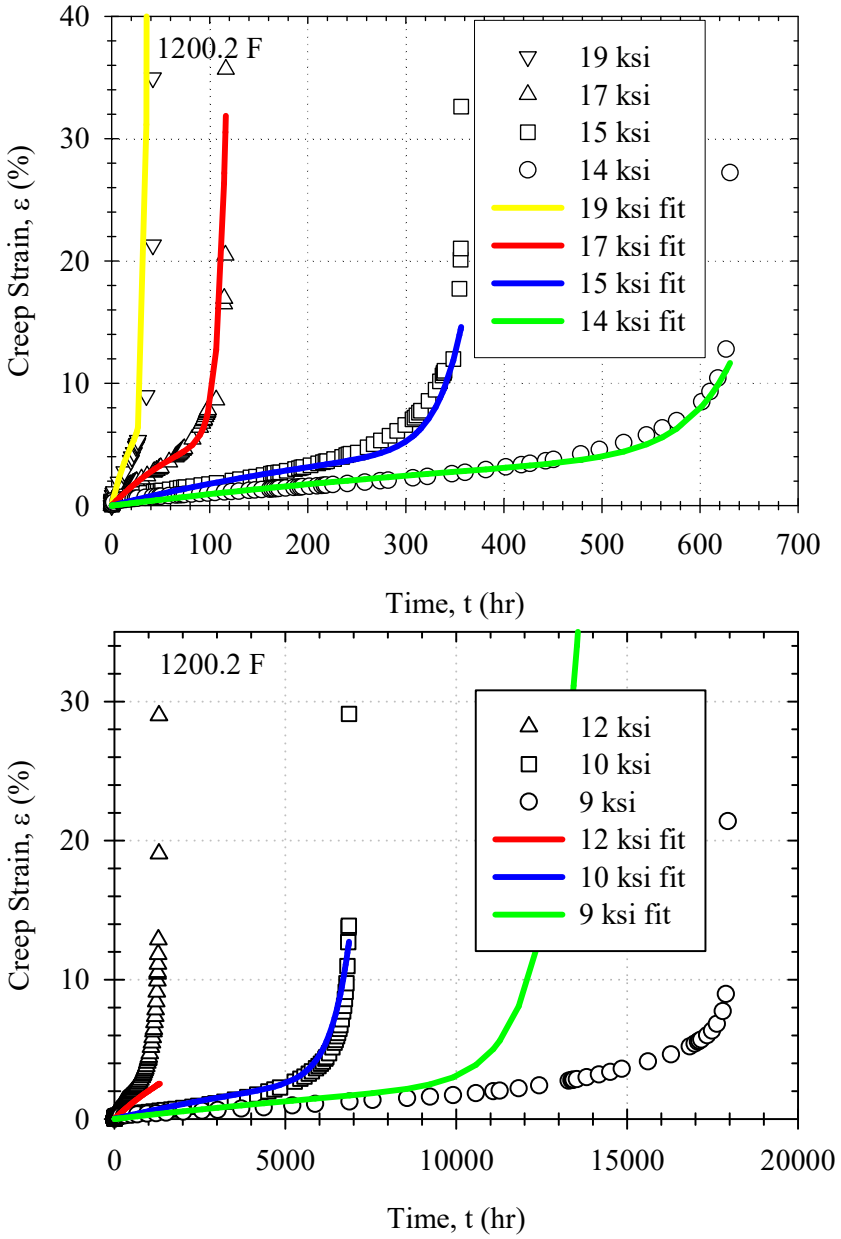

Figure 15.5: Predictions made using interpolated and extrapolated theta constants compared to data used in calibration.

4.5 ANALYTICAL CALIBRATION RESULTS

The process of calibration is repeated using the analytical technique. The values of θ_1, θ_2, θ_3 and θ_4 that are predicted as a result of calibration using the analytical technique are presented in Appendix Table 2. Comparing them to theta values in Appendix Table 1, it is evident that the two methods of calibration produce values of θ_1, θ_2, θ_3 and θ_4 that differ greatly. Examining

Appendix Table 2, a trend in theta constants can be identified. The values for θ_1, θ_2, θ_3 and θ_4 all descend as stress increases at a single isotherm. This trend reflects the behavior of the calibration data. Due to the nature of the analytical approach, the calibrated fits model a conservative representation of the data.

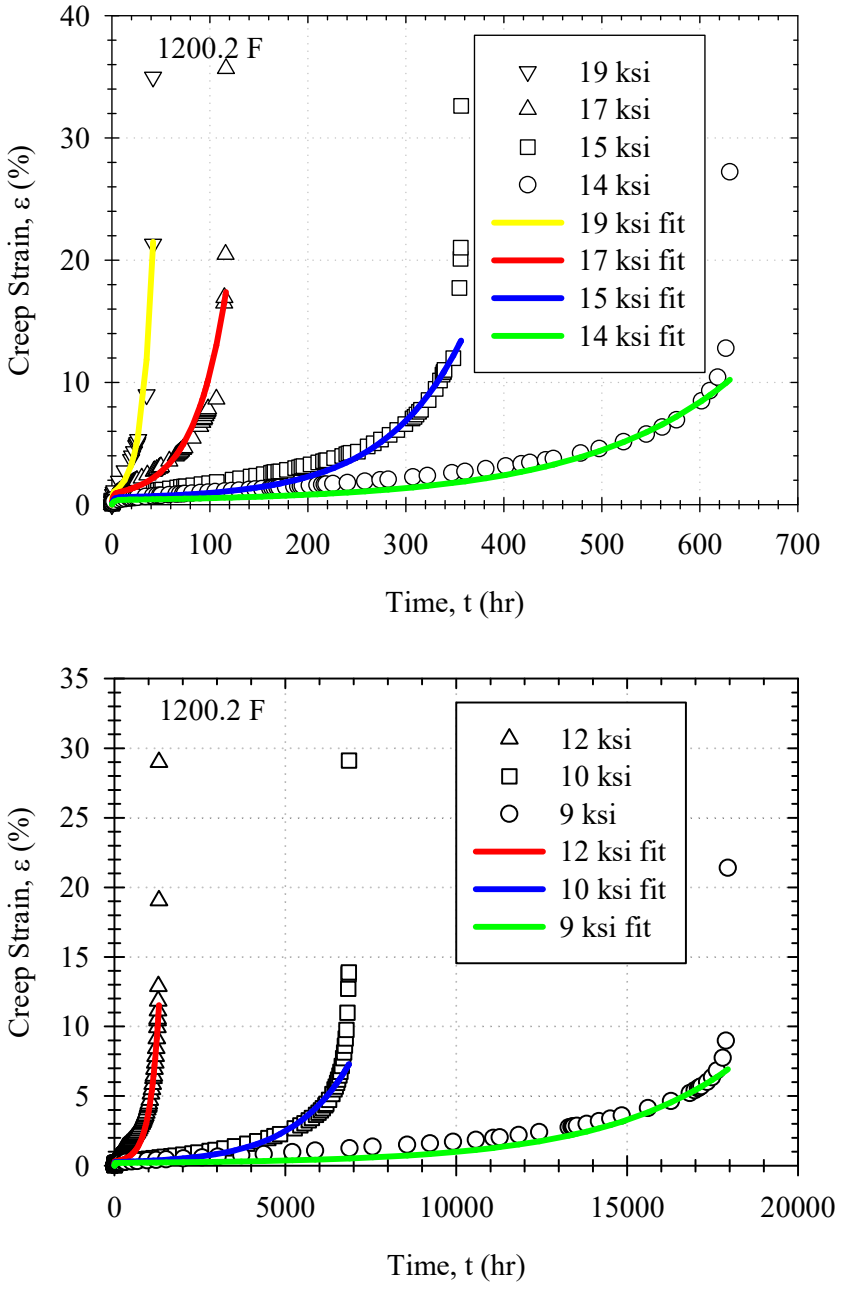

Figure 16.6: Calibrated fits to test data using the analytical method.

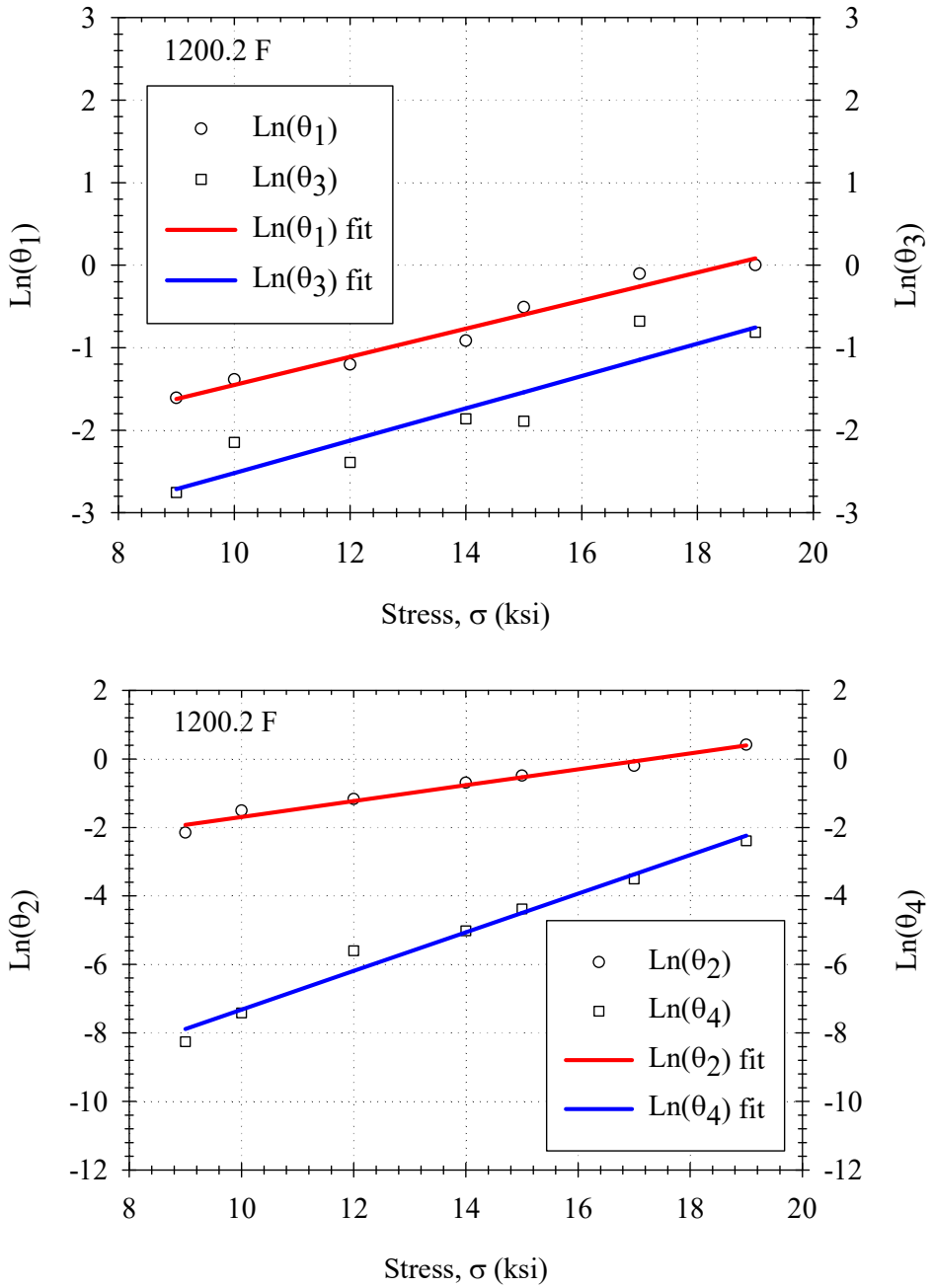

Figure 17.7: Theta constants calibrated using the analytical method.

Using values of θ_1, θ_2, θ_3 and θ_4 in Appendix Table 2, creep strain predictions are produced at 19-9 ksi all at 1200ºF. These predictions are compared to experimental data in Figure

18.8. Almost all predictions closely resemble the experimental, the only exceptions being those produced at 12 and 9 ksi. The prediction at 12 ksi underpredicts the rupture ductility. The prediction at 9 ksi predicts the full rupture ductility, but does not accurately predict the behavior to rupture when compared to experimental data. Comparing Figure 15.5 and Figure 18.8, it is evident that predictions resulting from calibration using the analytical technique are superior to those made using numerical optimization. Comparing the prediction error of both methods, the error of the problematic predictions at 19, 12 and 9 ksi in Table 3 are minimal in Table 4. Though they are still relatively larger compared to the errors of the other predictions, they are much more representative of experimental data.

Table 4 – Normalized mean square error comparison of calibrated fits and predictions made using the analytical technique.

Isostress	Calibration NMSE	Prediction NMSE
19 ksi	0.0267	0.2195
17 ksi	0.0506	0.0702
15 ksi	0.0885	0.0959
14 ksi	0.1458	0.1099
12 ksi	0.1673	0.3943
10 ksi	0.0947	0.1040
9 ksi	0.1703	9.0104

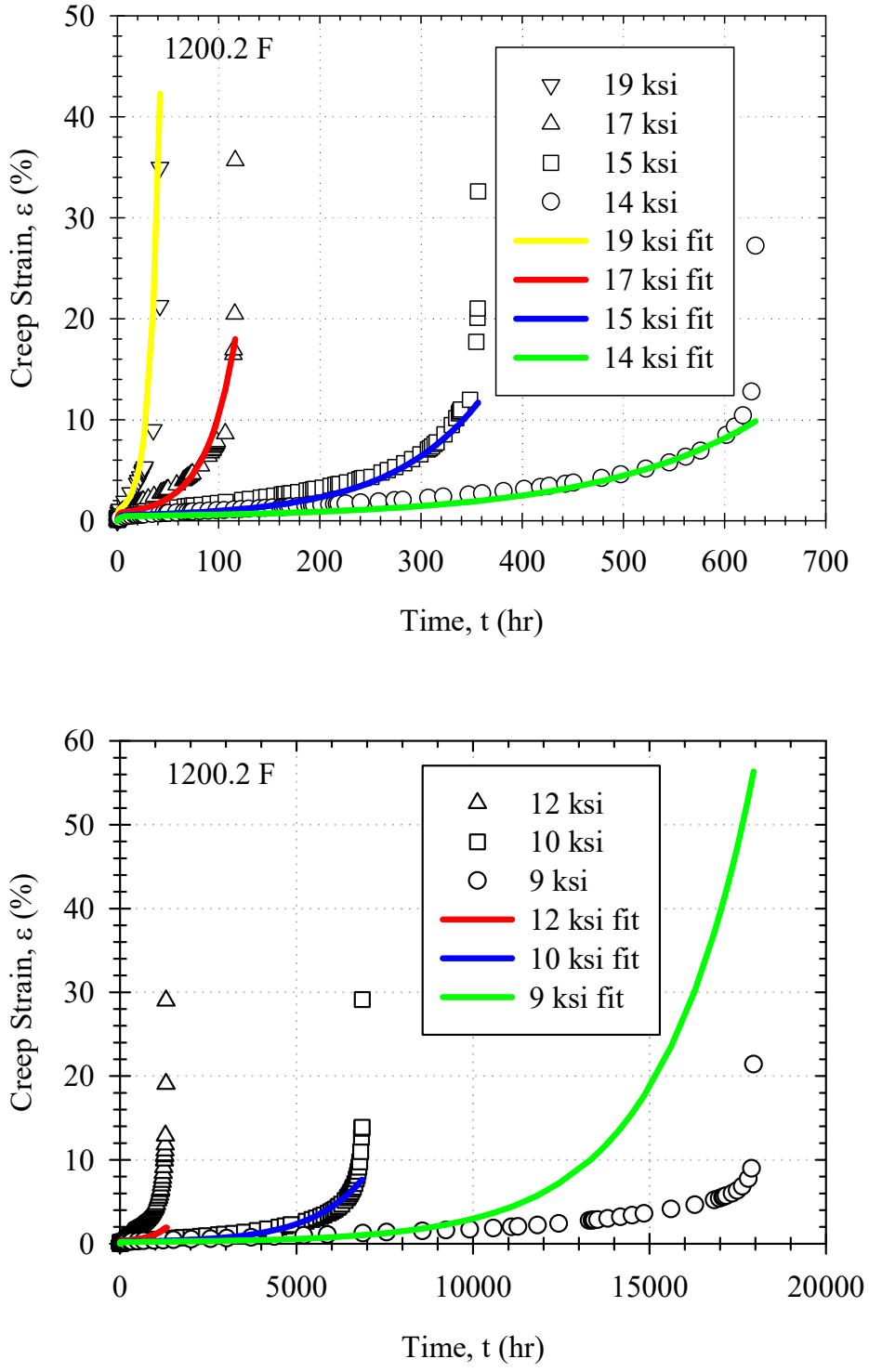

Figure 18.8: Predictions made using interpolated and extrapolated theta constants compared to data used in calibration.

4.6 CONCLUSIONS

The issues with calibration using numerical optimization stem from the inconsistency of calibrated theta constants from isostress to isostress. This inconsistency results in slight variations of predicted values of θ_1, θ_2, θ_3 and θ_4 when functionalized using [Eq.(14)] these variations have dramatic effect when used to predict the behavior of creep deformation. The resulting predictions vary drastically in quality, ranging from accurate to undesirable. When the analytical technique is used to calibrate the theta-projection model to the data, the resulting values of θ_1, θ_2, θ_3 and θ_4 maintain a realistic and consistent trend as stress decreases. This consistency in theta values produces much better predictions. Though similar issues arise in prediction when comparing both approaches to calibration, the quality of predictions resulting from the analytical calibration technique are much more reasonable. To address these remaining issues, it is necessary to functionalize calibrated theta values more accurately. An alternative interpolation/extrapolation function of different functional form from [Eq. (5)&(14)] may serve to fill this role.

CHAPTER 5: ALTERNATIVE INTERPOLATION/EXTRAPOLATION FUNCTION STUDY

5.1 INTRODUCTION

Although the analytical approach to calibration reduces the scatter in functionalized theta values, the original interpolation/extrapolation function experiences difficulty in fitting the calibrated constants. This results in excellent fits calibrated fits, but the interpolated/extrapolated predictions may not be consistent enough to be indicative of actual creep deformation behavior. To address this issue, a new interpolation/extrapolation function is explored.

A trend is identified in the rupture times of test data as stress increases. To utilize this trend, an alternative interpolation/extrapolation function that relies on rupture time rather than temperature and stress is used to establish a relationship between the calibrated theta constants and rupture time. Simulations, interpolations and extrapolations are made using both the original interpolation function as well as the alternative interpolation/extrapolation function and the results are compared qualitatively and quantitatively using the NMSE. It is found that the alternative function produces improved strain predictions, however to complete the model, it is necessary to provide a means of reliably predicting rupture time. The Wilshire method for creep prediction provides an equation to predict rupture time. It is found that, when calibrated correctly, the new technique of creep strain prediction using the Wilshire model for rupture time prediction produces prediction results that are on par with the original theta-projection model while requiring the use of fewer material constants.

5.2 NEW INTERPOLATION/EXTRAPOLATION FUNCTION

It is evident from the results of CHAPTER 4**: ANALYTICAL CALIBRATION TECHNIQUE**

that a more reliable method of interpolating and extrapolating theta constants from calibrated data is required to make better predictions. Observing the sets of experimental creep deformation data used in CHAPTER 1**: INTRODUCTION**

revealed a trend in the behavior of creep deformation until rupture with stress at every isotherm. The relationship of rupture time and each theta constant can be used to make interpolated/extrapolated predictions of strain. This relationship is as follows;

$$\theta_i = A_i(t_f)^{B_i} \tag{23}$$

where A and B are constants identified in calibration similar to the a, b, c, and d constants in [Eq. (5)&(14)] This alternate method of calibration serves to further relate θ_1, θ_2, θ_3 and θ_4 to experimental data and establish a physically realistic trend in prediction. The rupture time used in [Eq.(23)] is not the true rupture time of the experimental data, rather it is the last consistent time measurement recorded just before the material begins to fracture. The following study compares this new interpolation/extrapolation function to the original.

Material and data information

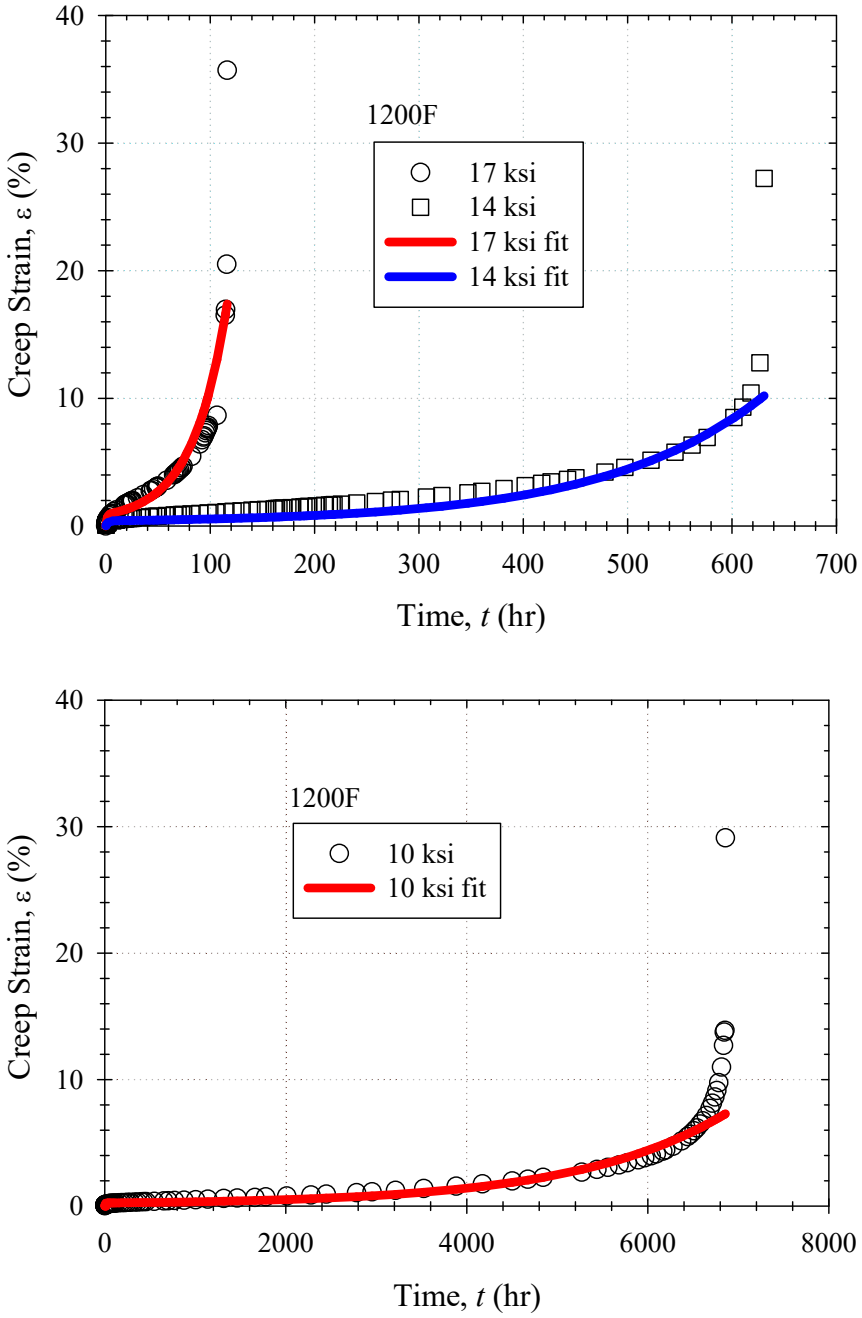

Figure 19.1: Calibrated theta constants using the analytical method to test data of alloy P91.

The material used in this study is alloy P91. The test data used in calibration was recorded at 3 different stresses (10, 14 and 17 ksi) at a single isotherm of 1200ºF. Analyzing multiple stresses at a single isotherm simplifies analysis. Data used in post-audit validation is 4 tests at 9, 12, 15 and

19 ksi all at 1200ºF. All data used in this study was collected by Oak Ridge National Laboratory [8]. An additional 10 points of creep rupture data are used to calibrate initial Wilshire material constants.

Calibration

The calibrated theta constants used in this study are found using the analytical technique discussed in CHAPTER 4: ANALYTICAL CALIBRATION TECHNIQUE

. The fits calibrated experimental data are illustrated in Figure 19. The limit in calibrated ductility is a result of the analytical technique, the conservative fit allows θ_1, θ_2, θ_3 and θ_4 to maintain a realistic trend as stress increases while fitting the data accurately.

Calibrated theta constants

The calibrated constants are functionalized using the original interpolation/extrapolation equation [Eq.(5)] in Figure 20.2, and the alternative interpolation/extrapolation function [Eq.(23)] in Figure 21.3. These plots serve to show the difference in prediction for interpolated and extrapolated values of theta.

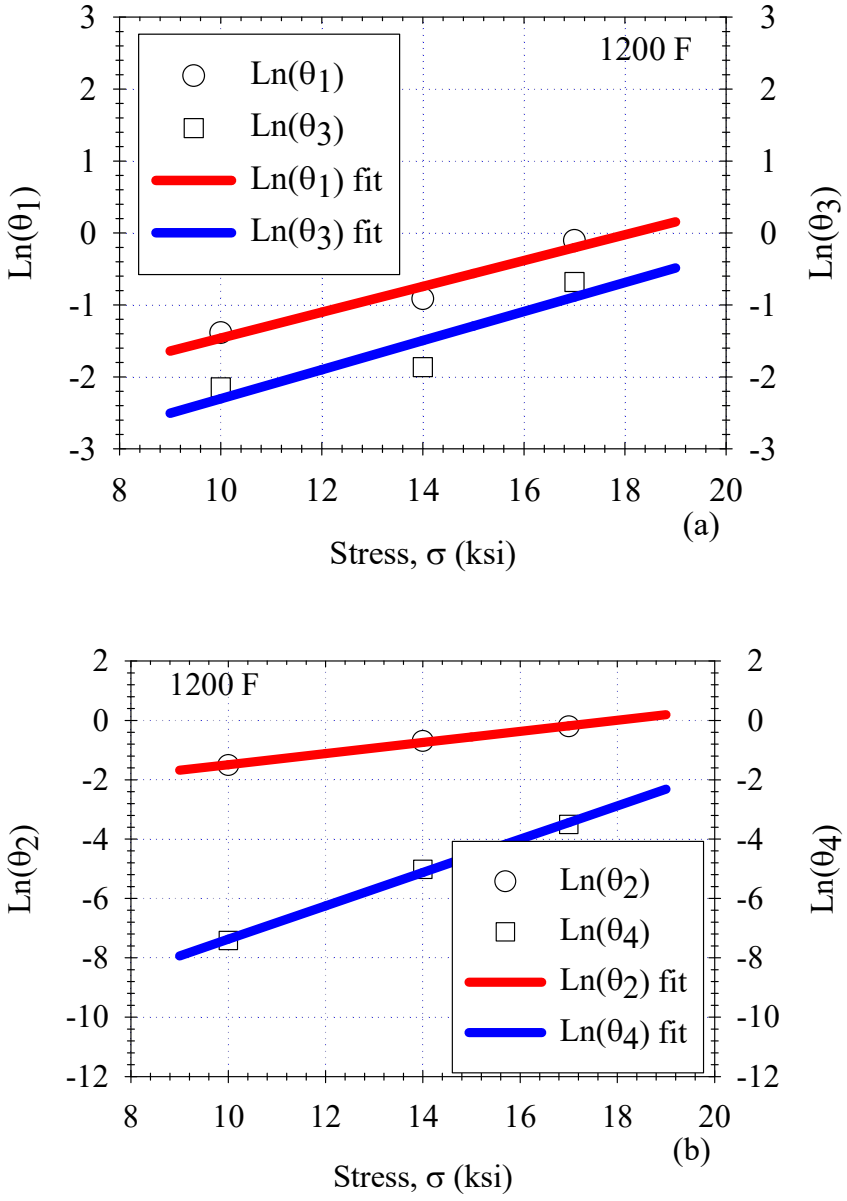

Figure 20.2: Calibrated θ_1, θ_2, θ_3 and θ_4 constants functionalized using the original interpolation/extrapolation equation.

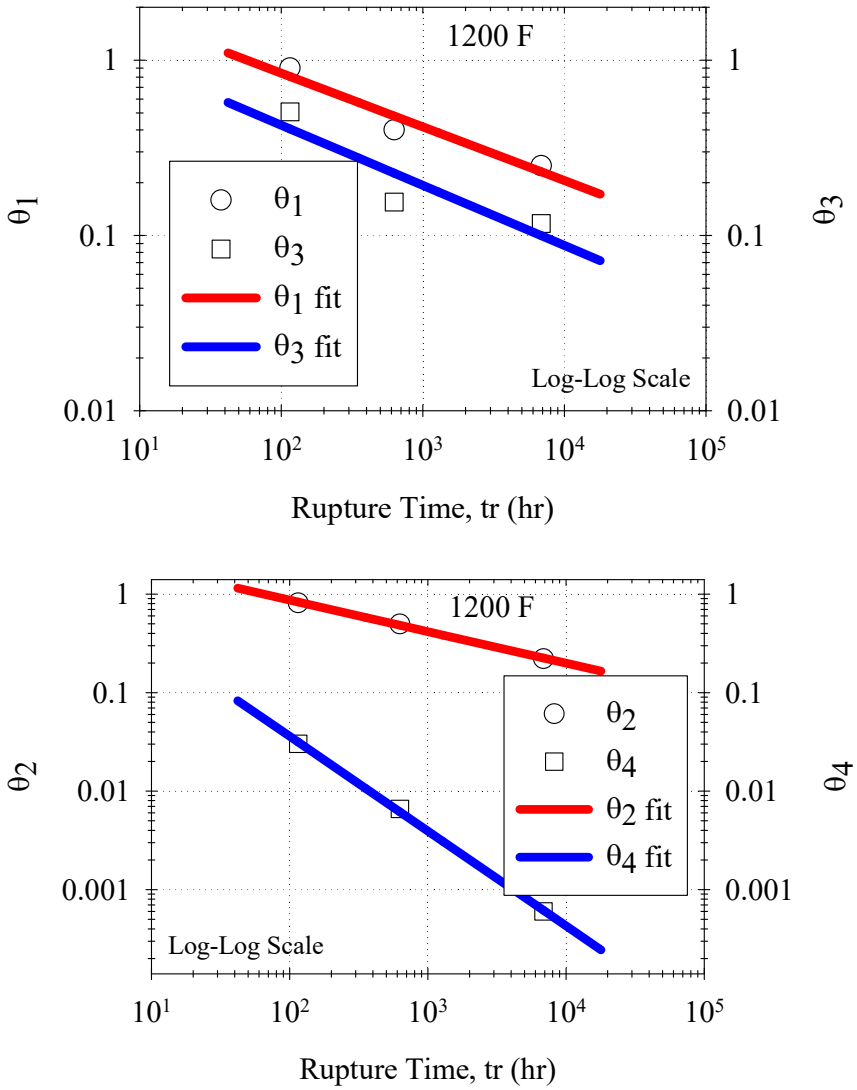

Figure 21.3: Calibrated θ_1, θ_2, θ_3 and θ_4 constants functionalized using the alternative interpolation/extrapolation equation.

5.3 RESULTS

Interpolations and Extrapolation

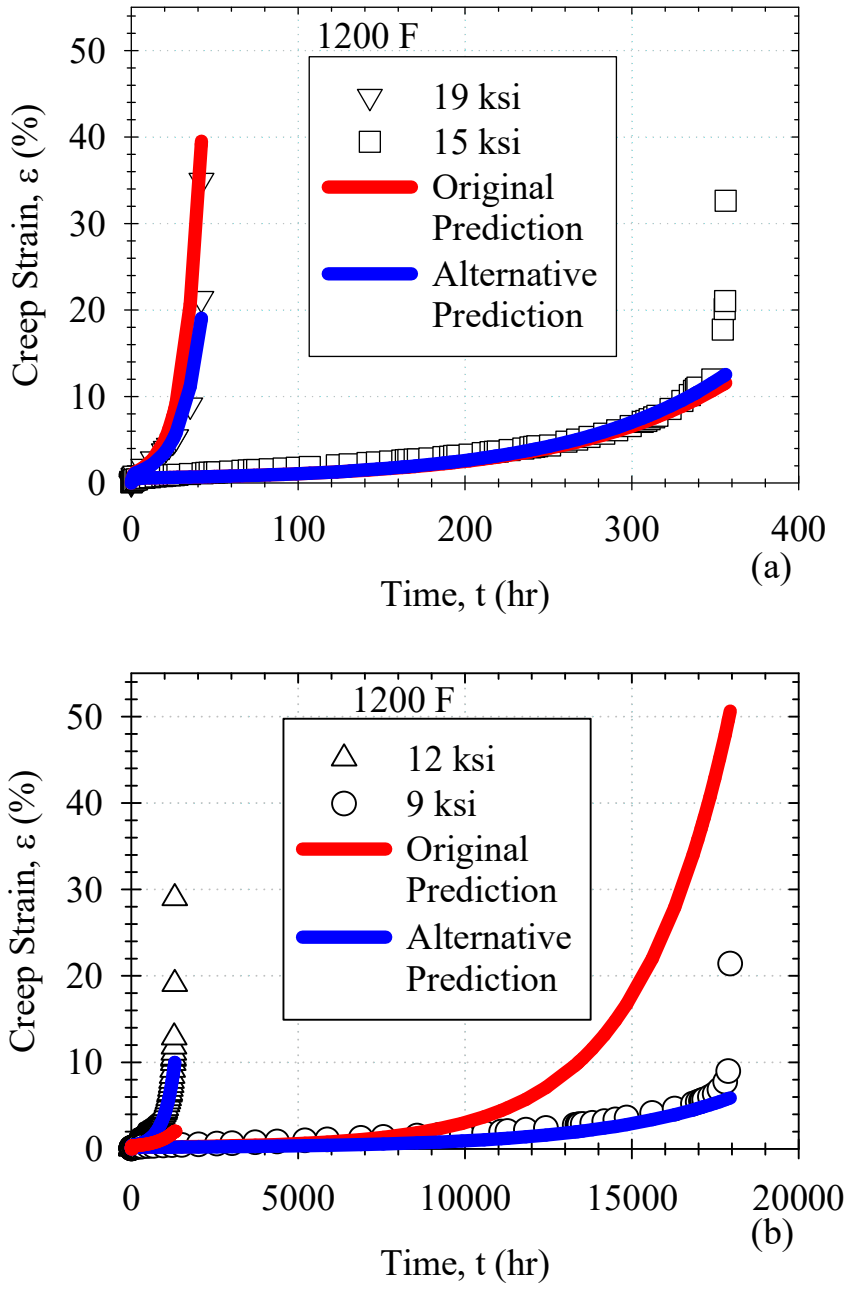

Figure 22.4: Interpolated and extrapolated predictions made using the alternative interpolation/extrapolation function compared to predictions made using the original interpolation/extrapolation function and validation data.

Predictions of creep deformation are made using both interpolation/extrapolation functions and are plotted together against validation data and is illustrated in Figure 22.4. It is evident that using [Eq.(5)] produces fits that vary drastically in quality. Prediction at 19 ksi is the best representation of prediction using the original function [Eq.(5)], modelling the curve well and depicting ductility similar to the validation data. Prediction at 12 ksi using [Eq.(5)] severely underpredicts the behaviour of creep deformation when compared to validation data and prediction at 9 ksi greatly overpredicts creep deformation. This shifting consistency is due to the nature of the interpolation/extrapolation equation. Small variances in theta values predicted using [Eq.(5)] result in a large shift in the way the creep curve will behave. The predictions made using the alternative function [Eq.(23)] maintain consistent behaviour in every instance. A comparison of the NMSE is illustrated in Table 5. From this table, the improvement in interpolated/extrapolated prediction of [Eq.(23)] over [Eq.(5)] can be seen quantitatively.

Table 5 – Normalized mean square error comparison of interpolated/extrapolated predictions using Eq. 2 and Eq. 3 to validation data.

Stress	NMSE of predictions using $\theta_i = \exp(a_i + b_i\sigma + c_iT + d_i\sigma T)$	NMSE of predictions using $\theta_i = A_i(t_r)^{-B_i}$
19 ksi	0.232787	0.030612
15 ksi	0.078304	0.070085
12 ksi	0.372753	0.095080
9 ksi	7.428862	0.190037

5.4 DISCUSSION

It is evident from Table 5 that the predictions made using the alternative interpolation/extrapolation function [Eq.(23)] are quantitatively better in every instance.

Analyzing the prediction plots in Figure 22.4, the following conclusions can be drawn: The more data used in calibration, a more consistent trend in θ_1, θ_2, θ_3 and θ_4 can be derived using the original function [Eq.(5)]. When limited data is used in calibration, the trends established in θ_1, θ_2, θ_3 and θ_4 do not allow for accurate strain predictions for all stress conditions at a single isotherm. When using [Eq.(23)], it is apparent that the relationship of theta constants to rupture time allows for more consistent and accurate predictions to be made, even when limited data is used in calibration. It should be noted that when using the analytical approach to calibration, the predictions do not depict the full ductility of the validation data. This results in conservative predictions of strain with time which may be useful in design.

Due to [Eq.(23)] relying on approximate rupture time rather than temperature and stress, it is necessary to predict the rupture time of a test specimen. The Wilshire model provides a means to analytically determine the rupture time of a test [9-[*12*]. Using the Wilshire model to predict rupture time with the alternative interpolation/extrapolation function used in this study and the analytical approach to calibration, a new method for applying the theta projection model may be developed.

5.5 WILSHIRE RUPTURE PREDICTIONS

Wilshire Rupture Predictions

The Wilshire approach to creep prediction is a time dependent model that is able to predict creep rupture and minimum creep strain rate at multiple isotherms [[*9*-[*12*]. Of particular interest for inclusion into the modified theta application is Wilshire creep rupture interpolation/extrapolation equation. The rupture interpolation/extrapolation equation is as follows

$$\frac{\sigma}{\sigma_{TS}} = \exp\left(-k_1 \left[t_f \exp\left(-\frac{Q_c^*}{RT} \right) \right]^u \right) \tag{24}$$

where σ and σ_{TS} are the stress of the creep test and ultimate tensile stress (UTS) of the material respectively, Q is the activation energy of the material, T is the temperature of the creep test, R is the universal gas constant, t_f is the final or rupture time of the creep test and both k_1 and u are material constants. The reliance on temperature and stress and UTS of the material allow for excellent rupture time predictions which is exactly what is needed to finish the alternative theta projection method. Rewriting [Eq.(24)] becomes

$$t_f = \left[\frac{\ln\left(\frac{\sigma}{\sigma_{TS}} \right)}{-k_1} \right]^{\frac{1}{u}} \frac{1}{\exp\left(\frac{-Q_c^*}{RT} \right)} \tag{25}$$

allowing rupture time to be solved for when the appropriate conditions are used.

Using k_1 and u, calibrated to the sets of creep deformation data in Figure 3, rupture times are predicted using temperature-stress parameters of 1200ºF and 19, 15, 12, and 9 ksi with [Eq.(24)] [12]. These rupture predictions are plotted against 10 points of creep rupture data to show the quality of fit through the data. Using these predictions with the alternative interpolation function [Eq.(23)] new theta constants are derived for use in making interpolated and extrapolated predictions of creep strain. The derived theta constants as well as the rupture predictions and corresponding conditions are illustrated in Appendix Table 3.

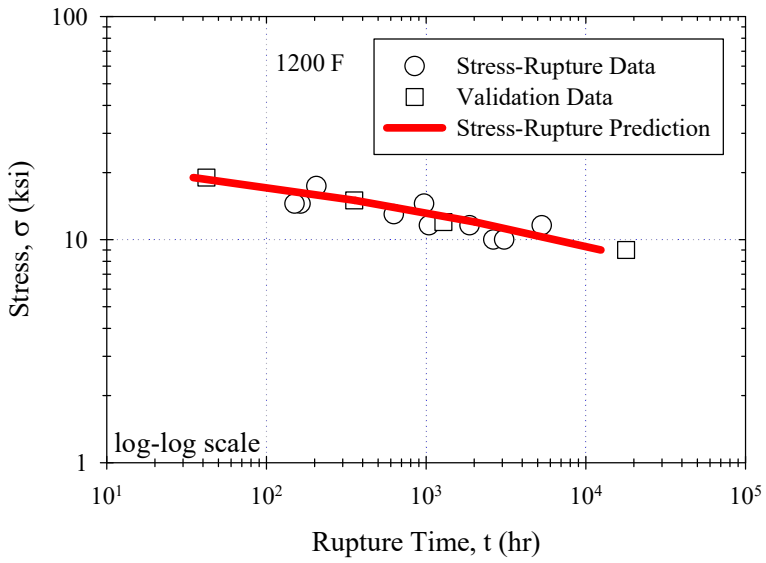

Figure 23.5: Rupture time predictions made using k_1, and u in Table 2.

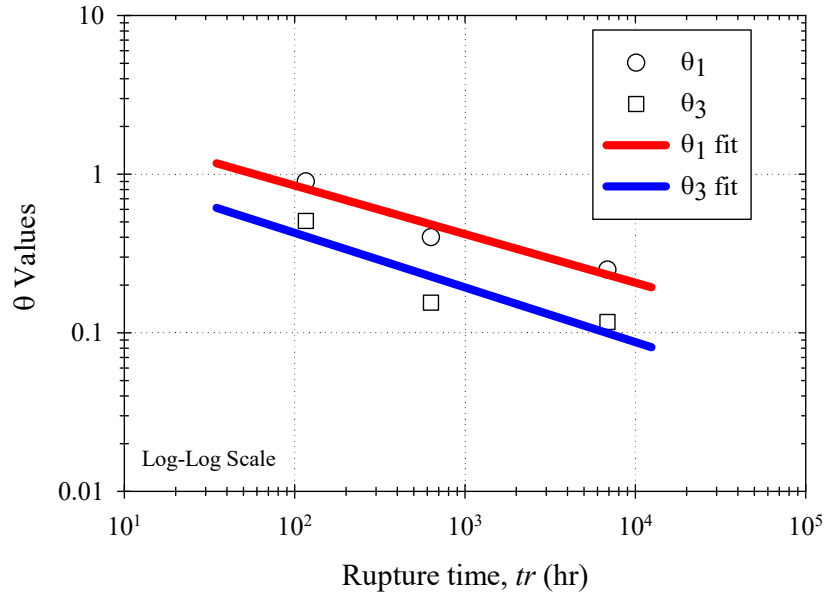

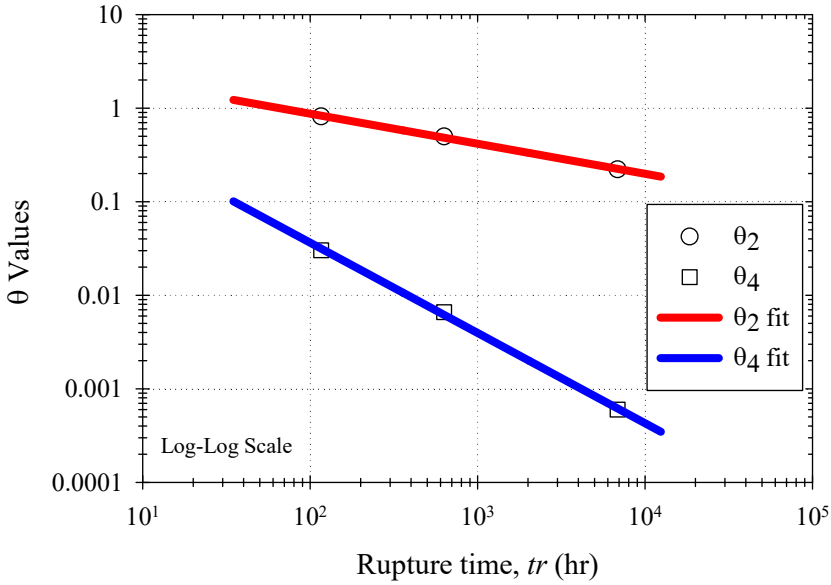

Figure 24.6: Calibrated θ_1, θ_2, θ_3 and θ_4 values plotted against calibrated θ_1, θ_2, θ_3 and θ_4 values.

The principal benefit of using the Wilshire model to predict rupture time is that it draws from the data used to calibrate k_1 and u to produce realistic rupture times. Traditional method of

rupture prediction used with the theta-projection model relies on an additional equation to predict rupture strain

$$\varepsilon_f = a + bT + c\sigma + d\sigma T \tag{26}$$

where *a*, *b*, *c* and *d* are constants that themselves require calibration while σ and *T* correspond to the desired conditions of interpolation/extrapolation [2-4]. Once the rupture strain is predicted, it is used with [Eq.(2)] to determine rupture time [2-4]. This requires θ_1, θ_2, θ_3 and θ_4 for the appropriate interpolated/extrapolated σ and *T*, which necessitates calibration of a_i, b_i, c_i and d_i for the interpolation/extrapolation equation [Eq.(5)]. This totals to 20 distinct constants that require calibration using the theta-projection method whereas the Wilshire method requires only 10. The 10 constants being k_1, u, A_i and B_i where $i = 1-4$. In Figure 25.7, the times to rupture used to make interpolated and extrapolated predictions using the original function are found by taking the average rupture strain of P91 data at 1200ºF and using the aforementioned technique of back-solving [Eq.(2)] for rupture time. The average rupture strain of P91 data at 1200ºF is 8% strain, the rupture times are listed below in Table 7.

Results

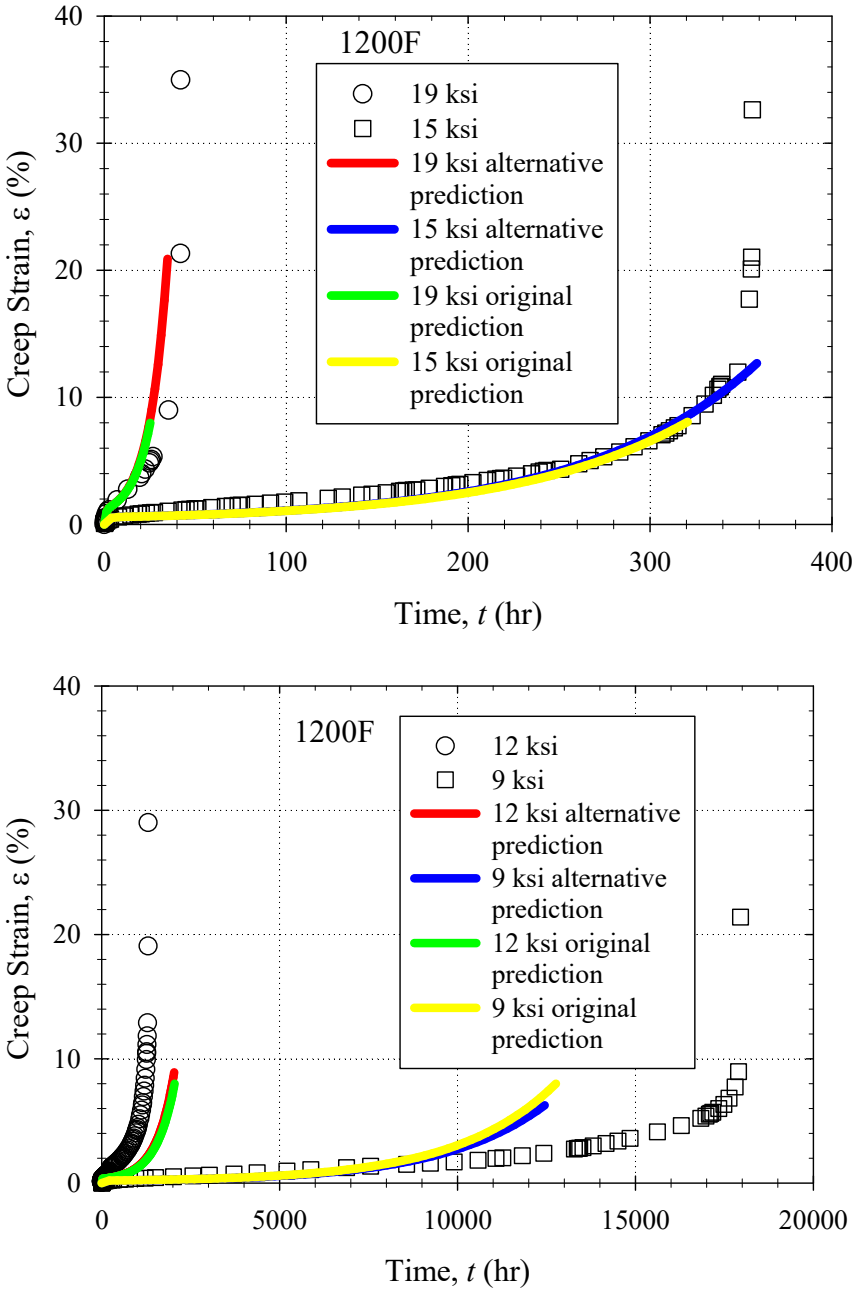

Figure 25.7: Interpolated and extrapolated predictions of creep strain made using theta constants in Appendix Table 3.

Interpolated and extrapolated predictions of creep strain are made using the theta constants derived with [Eq.(23)], presented in Appendix Table 3. The quality of the predictions is reasonable.

Nearly all interpolated predictions depict ductility better than predictions made using the original interpolation/extrapolation function [Eq.(5)]. The only exception being the extrapolation at 9 ksi. The NMSE of both predictions at each isostress is illustrated in Table 6. The predictions on par with those made using the original theta-projection method [Eq.(5)]. The similar error means that while the original method is not surpassed by any significant margin, using Wilshire rupture time predictions with [Eq.(25)] is a viable alternative for creep strain prediction using the modified theta-projection approach.

Table 6 – Interpolated and extrapolated predictions made using the original and alternative functions and their NMSE compared to validation data at 19, 15, 12, and 9 ksi, all at 1200ºF.

Prediction at stress level	NMSE of prediction using original interpolation/extrapolation function	NMSE of prediction using alternative interpolation/extrapolation function
19 ksi	2.4733	3.8565
15 ksi	0.5551	0.5116
12 ksi	0.7364	0.7593
9 ksi	1.8113	1.8066

Table 7 – Rupture times at 8% strain calculated using [Eq.(2)] to make interpolated/extrapolated creep predictions.

Predictions at stress	Rupture times at 8% strain
19 ksi	25.2332 hrs
15 ksi	320.672 hrs
12 ksi	2046.90 hrs
9 ksi	12765.7 hrs

Results Note

Before the results were generated, a broader range of creep rupture data was used to calibrate k_1 and u while the data from Figure 19.1 was used to calibrate A and B. This resulted in predictions that were not as good as those in Figure 25.7. It is necessary that the same calibration data be used for all constants in the modified theta-projection method.

5.6 CONCLUSIONS

The modified method for applying the theta-projection model is a viable alternative to the original proposed by Evans. When using the same rupture time in generating interpolated and extrapolated predictions of creep deformation, the alternative interpolation/extrapolation equation out-performs the original interpolation/extrapolation equation. The quality of predictions made using Wilshire derived rupture times varies depending on calibration. Using a broad set of data to calibrate Wilshire constants but using a smaller range for calibrating theta constants results in predictions that are not as good as those produced using the theta-projection techniques. When the same test data is used to calibrate both the Wilshire constants and theta-projection constants, the resulting predictions of creep deformation behavior are on par with those produced using the traditional theta-projection method. The modified theta-projection method is a viable alternative to the original. The benefit is that the modified method is a purely analytical approach that requires fewer constants to be calibrated.

Future Work

There are several avenues to further assess the validity of the modified theta-projection technique. The first of which is to expand the study by examining the performance of the modified technique when applied to multiple isotherms. It would be interesting to see how this the modified model fares at conditions of temperature and stress suited to different areas of power generation.

While 1200ºF is a typical temperature for ultra-supercritical coal-fired power plants, turbines in more commonplace coal-fired power plants are subject to temperatures from 1100ºF to 800ºF. Examining the behavior of the modified technique at these isotherms at multiple stress levels would provide evidence for the applicable range of the method.

Another direction for continuing the assessment of the modified method is to apply the method in computational mechanics. Examining the simulated strain-life prediction capability of the model when applied to the geometry of turbine blades lends more validity to its application in industry.

CHAPTER 6: CONCLUSIONS

6.1 REVIEW

Chapter 3

The theta-projection model excels at fitting shape of all three regimes of creep deformation. The model has the ability to make interpolated and extrapolated predictions of creep deformation derived from calibration. The initial issue lies in the method used to calibrate the model to experimental data. The numerical optimization process yields excellent fits to experimental data. When interpolating theta constants using [Eq.(5)] however, the predicted constants used in conjunction with one another do not always yield accurate predictions. This variation results from the nature of numerical optimization. When the error-dependent least-square non-linear scheme determines values for θ_1, θ_2, θ_3 and θ_4, the values may not necessarily follow a realistic trend relative to the data they are being fitted to. This lack of a realistic behavior results in predicted values of θ_1, θ_2, θ_3 and θ_4 that are not compatible with one another and thus produce inaccurate predictions of creep deformation.

Chapter 4

Establishing a trend in theta constants with temperature and stress is important to make better interpolated/extrapolated predictions. The analytical method of calibration establishes a realistic trend in theta constants with temperature and stress. The analytically calibrated constants allow for better prediction than numerically optimized constants. Despite this improved prediction, the accuracy of several interpolations and extrapolation is not reasonable. To improve prediction accuracy, a new interpolation/extrapolation function may better serve to fit the calibrated constants better than [Eq. (5)].

Chapter 5

A new interpolation/extrapolation function is introduced relating theta constants to rupture time rather than temperature and stress. The new interpolation/extrapolation function is of different mathematical form and when calibrated correctly it produces better interpolated and extrapolated predictions than the original. An equation from the Wilshire method is used to predict rupture time for the new interpolation/extrapolation function, completing an alternative method of prediction using the theta-projection model. This new method I compared to the traditional method of theta-projection and is found to produce predictions that are on par with the traditional method. A benefit to using the alternative method is that it requires less constants to be calibrated than the traditional method.

6.2 CONCLUSIONS

Using the analytical technique for calibration, the new interpolation/extrapolation function, and the Wilshire method for predicting rupture time, all together becomes an alternative method of calibration and prediction for the theta-projection model. The alternative method overcomes the shortcomings of the original theta-projection method. The analytical approach provides better calibration and generates more consistent theta constants with one another than numerical

optimization. The new interpolation/extrapolation function produces more accurate predictions than the original. Using the Wilshire equation to predict rupture time, the predictions are on par with those made using the traditional method of rupture time prediction with the theta model. The entire modified theta-projection approach provides a concise systematic method for calibration and prediction that uses less constants than the original theta method. The alternative theta method is a viable and beneficial alternative.

Future Work

There are several modified forms of the theta projection model developed to improve accuracy and apply it to different material and conditions, the most notable being a 6-theta equation developed by Evans to better fit the primary range of low strain tests [[*27*-[*33*]. Several of these serve to better fit certain creep regimes, application of these techniques will increase accuracy beyond that of the original theta-projection model. It would also be interesting to introduce or evaluate existing theta-projection models that have a separate function for the secondary creep regime. Applying these techniques with the proposed analytical method for calibration may serve to further increase accuracy in interpolated and extrapolated creep predictions.

Using the alternative method of calibration and for the theta-projection model to make predictions at temperatures other than 1200ºF such as those used in CHAPTER 3: THETA-PROJECTION PERFORMANCE REVIEW

. Using creep test data at different temperatures and stresses to calibrate and make interpolated/extrapolated predictions grants the opportunity to see how the modified theta method behaves at different conditions. In the proposition for future work in CHAPTER 5: ALTERNATIVE INTERPOLATION/EXTRAPOLATION FUNCTION STUDY

, applying the modified method to computational mechanics was discussed. The modified method can be applied to the simulated geometry of turbine blades, steam tubes, and other critical components of power generation to assess their behavior when subject to creep strain.

The reality of creep is that it exhibits uncertainty. At identical conditions of temperature and stress, each creep test behaves differently [[*34*-[*35*]. The Alternative method of application and prediction for the theta-projection model is applied deterministically and does not account for uncertainty. Altering the alternative theta-projection method to apply it as a stochastic model increases its potential and viability. Incorporating the use of Monte Carlo simulation in the alternative theta-projection method may serve to further that end.

Acknowledgments

This material is based upon work supported by the Department of Energy National Energy Technology Laboratory under Award Number(s) DE-FE0027581.

REFERENCES

[1] Haque, M. S., & Stewart, C. M. (2019). The disparate data problem: the calibration of creep laws across test type and stress, temperature, and time scales. Theoretical and Applied Fracture Mechanics.

[2] Sawada, K., Tabuchi, M., & Kimura, K. (2009). Analysis of long-term creep curves by constitutive equations. Materials Science and Engineering: A, 510, 190-194.

[3] Haque, M. S., & Stewart, C. M. (2016, July). Exploiting Functional Relationships Between MPC Omega, Theta, and Sinh-Hyperbolic Continuum Damage Mechanics Model. In ASME 2016 Pressure Vessels and Piping Conference (pp. V06AT06A052-V06AT06A052). American Society of Mechanical Engineers.

[4] Evans, R. W., & Wilshire, B. (1985). Creep of metals and alloys.

[5] Brown, S. G. R., Evans, R. W., & Wilshire, B. (1986). A comparison of extrapolation techniques for long-term creep strain and creep life prediction based on equations designed to represent creep curve shape. International Journal of Pressure Vessels and Piping, 24(3), 251-268.

[6] Brown, S. G. R., Evans, R. W., & Wilshire, B. (1986). Creep strain and creep life prediction for the cast nickel-based superalloy IN-100. Materials Science and Engineering, 84, 147-156.

[7] Evans, R. W., Parker, J. D., & Wilshire, B. (1992). The θ projection concept—A model-based approach to design and life extension of engineering plant. International Journal of Pressure vessels and piping, 50(1-3), 147-160.

[8] Wilshire, B., & Battenbough, A. J. (2007). Creep and creep fracture of polycrystalline copper. Materials science and engineering: a, 443(1-2), 156-166.

[9] Wilshire, B., & Scharning, P. J. (2007). Long-term creep life prediction for a high chromium steel. Scripta Materialia, 56(8), 701-704.

[10] Wilshire, B., & Scharning, P. J. (2008). Prediction of long term creep data for forged 1Cr–1Mo–0· 25V steel. Materials science and technology, 24(1), 1-9.

[11] Cano, J.A, & Stewart, C.M (2019). Application of the Wilshire Stress-rupture and Minimum-Creep-Strain-Rate Prediction Models for Alloy P91 in Tube, Plate and Pipe Form. ASME Turbo Expo 2019: Turbomachinery Technical Conference and Exposition Phoenix, Arizona.

[12] Evans, M. (2012). A new statistical framework for the determination of safe creep life using the theta projection technique. Journal of Materials Science, 47(6), 2770-2781.

[13] Shibli, A., & Starr, F. (2007). Some aspects of plant and research experience in the use of new high strength martensitic steel P91. International journal of pressure vessels and piping, 84(1-2), 114-122.

[14] Oak Ridge National Laboratories, "Materials Handbook for Generation IV Reactors." https://gen4www.ornl.gov/.

[15] Andrade, E. N. D. C. (1910). On the viscous flow in metals, and allied phenomena. Proceedings of the Royal Society of London. Series A, Containing Papers of a Mathematical and Physical Character, 84(567), 1-12.

[16] Betten, J., 2002, Creep Mechanics, Springer.

[17] Betten, J. (2008). Creep mechanics. Springer Science & Business Media.

[18] Evans, M. (2002). Sensitivity of the theta projection technique to the functional form of the theta interpolation/extrapolation function. Journal of materials science, 37(14), 2871-2884.

[19] Evans, M. (2000). Predicting times to low strain for a 1CrMoV rotor steel using a 6-θ projection technique. Journal of materials science, 35(12), 2937-2948.

[20] Evans, M. (2002). The application of a new and robust weighting scheme for establishing theta projection parameters to 1CrMoV rotor steel. The Journal of Strain Analysis for Engineering Design, 37(2), 169-183.

[21] Evans, M. (2004). A comparative assessment of creep property predictions for a 1CrMoV rotor steel using the CRISPEN, CDM, Omega and Theta projection techniques. Journal of materials science, 39(6), 2053-2071.

[22] Evans, R. W., & Scharning, P. J. (2001). The θ projection method applied to small strain creep of commercial aluminium alloy. Materials science and technology, 17(5), 487-493.

[23] Pandey, C., Mahapatra, M. M., Kumar, P., & Saini, N. (2018). Some studies on P91 steel and their weldments. Journal of Alloys and Compounds, 743, 332-364.

[24] Kimura, K., Kushima, H., & Sawada, K. (2009). Long-term creep deformation property of modified 9Cr–1Mo steel. Materials Science and Engineering: A, 510, 58-63.

[25] Pandey, C., Mahapatra, M. M., Kumar, P., & Saini, N. (2017). Effect of creep phenomena on room-temperature tensile properties of cast & forged P91 steel. Engineering Failure Analysis, 79, 385-396.

[26] Hald, J. (2008). Microstructure and long-term creep properties of 9–12% Cr steels. International Journal of Pressure Vessels and Piping, 85(1-2), 30-37.

[27] Kariya, Y., Otsuka, M., & Plumbridge, W. J. (2003). The constitutive creep equation for a eutectic Sn-Ag alloy using the modified theta-projection concept. Journal of Electronic Materials, 32(12), 1398-1402.

[28] Kumar, M., Singh, I. V., Mishra, B. K., Ahmad, S., Rao, A. V., & Kumar, V. (2016). A modified theta projection model for creep behavior of metals and alloys. Journal of Materials Engineering and Performance, 25(9), 3985-3992.

[29] Day, W. D., & Gordon, A. P. (2013, June). A Modified Theta Projection Creep Model For A Nickel-Based Super-Alloy. In ASME Turbo Expo 2013: Turbine Technical Conference and Exposition (pp. V07AT26A002-V07AT26A002). American Society of Mechanical Engineers.

[30] Day, W. D., & Gordon, A. P. (2014, June). Life fraction hardening applied to a modified theta projection creep model for a nickel-based super-alloy. In 2014 Proceedings of the ASME Turbo Expo 2014: Turbine Technical Conference and Exposition, American Society of Mechanical Engineers (p. V07AT29A010).

[31] Alipour, R., & Nejad, A. F. (2016). Creep behaviour characterisation of a ferritic steel alloy based on the modified theta-projection data at an elevated temperature. International Journal of Materials Research, 107(5), 406-412.

[32] *Zhao, Y., Gong, J., Yong, J., Wang, X., Shen, L., & Li, Q. (2016). Creep behaviours of Cr25Ni35Nb and Cr35Ni45Nb alloys predicted by modified theta method.* Materials Science and Engineering: A*,* 649*, 1-8.*

[33] *Song, M., Xu, T., Wang, Q., Wang, W., Zhou, Y., Gong, M., & Sun, C. (2018). A modified theta projection model for the creep behaviour of creep-resistant steel.* International Journal of Pressure Vessels and Piping*,* 165*, 224-228.*

[34] Harlow, D.G. and Delph, T. J. "Creep Deformation and Failure : Effects of Randomness and Scatter." Journal of Engineering Materials and technology Vol. 122 No. 3 2000: pp. 342–347.

[35] Hayhurst, D. R. (1974). The effects of test variables on scatter in high-temperature tensile creep-rupture data. International Journal of Mechanical Science, 16(11), 829–840. https://doi.org/10.1016/0030-7403(74)90041-1

APPENDIX

Appendix Table 1 – Theta values predicted using [Eq.(5)] at 19-9 ksi and at 1200ºF, calibrated using numerical optimization.

Stress (ksi)	θ_1	θ_2	θ_3	θ_4
19	8.826866	0.040349	4.85E-06	0.437228
17	7.813086	0.011014	7.31E-06	0.129782
15	6.91574	0.003006	1.1E-05	0.038523
14	6.506489	0.001571	1.35E-05	0.020988
12	5.759208	0.000429	2.04E-05	0.00623
10	5.097754	0.000117	3.07E-05	0.001849
9	4.796085	6.11E-05	3.77E-05	0.001007

Appendix Table 2 – Theta values predicted using [Eq.(14)] at 19-9 ksi and at 1200ºF, calibrated the analytical technique.

Stress (ksi)	θ_1	θ_2	θ_3	θ_4
19	1.085022	1.486612	0.470011	0.106778
17	0.771669	0.934728	0.317652	0.034493
15	0.548812	0.587723	0.214681	0.011142
14	0.462828	0.466032	0.176488	0.006333
12	0.329164	0.293024	0.119278	0.002046
10	0.234102	0.184243	0.080613	0.000661
9	0.197424	0.146095	0.066271	0.000376

Appendix Table 3 – Calibrated Wilshire parameters with the resulting rupture time predictions and corresponding theta constant values, all at 1200ºF.

Wilshire constants	Stress σ, ksi	Rupture time t_r, hr	θ_1	θ_2	θ_3	θ_4
k_1	19	12448.6795	1.1714	1.2235	0.6137	0.1007
42.77	15	2032.6717	0.5734	0.5783	0.2749	0.0106
u	12	358.7839	0.3373	0.3314	0.1514	1.9941e-3
0.1184	9	34.7524	0.1937	0.1852	0.0812	3.4755e-4

VITA

My name is Jimmy Jesus Perez. I have earned my Bachelors degree in mechanical engineering (BSc in ME, 4 year degree) from the University of Texas at El Paso (UTEP). I have completed my degree requirement for Masters in mechanical engineering here at University of Texas El Paso. This thesis is submitted as a requirement of the degree including my research works throughout my graduate level study under the supervision of Dr. Calvin M Stewart.

Contact Information:

Jimmy Jesus Perez, email: jjperez3@miners.utep.edu